Swine H1N1 influenza virus variants with enhanced polymerase activity and HA stability promote airborne transmission in ferrets

Meng Hu[1], Jeremy C. Jones[1], Balaji Banoth[1], Chet Raj Ojha[1], Jeri Carol Crumpton[1], Lisa Kercher[1], Robert G. Webster[1], Richard J. Webby[1, 2], and Charles J. Russell[1, 2]

[1]Department of Infectious Diseases, St. Jude Children's Research Hospital, 262 Danny Thomas Place, Memphis, Tennessee 38105-3678, [2]Department of Microbiology, Immunology & Biochemistry, College of Medicine, The University of Tennessee Health Science Center, Memphis, Tennessee 38163.

Running Title: Polymerase activity and HA stability in influenza transmission

*** Corresponding author at:** Department of Infectious Diseases, MS 330, St. Jude Children's Research Hospital, 262 Danny Thomas Place, Memphis, TN 38105-3678, USA. Phone: 901-595-5648. Fax: 901-595-8559. Email: charles.russell@stjude.org.

Keywords: Influenza A virus / swine viruses / polymerase / viral fusion protein / transmissibility / virus adaptation

ABSTRACT

Understanding how animal influenza A viruses (IAVs) acquire airborne transmissibility in humans and ferrets is needed to prepare for and respond to pandemics. Here, we investigated the replication and transmission in ferrets of swine H1N1 isolates P4 and G15, whose majority population had decreased polymerase activity and poor HA stability, respectively. For both isolates, a minor variant was selected and transmitted in ferrets. Polymerase-enhancing variant PA-S321 was selected in half of P4 isolates that airborne-transmitted in ferrets. HA-stabilizing variant HA1-S210 was selected in all G15-inoculated ferrets and was transmitted by contact and airborne routes. With an efficient polymerase and a stable HA, the purified minor variant G15-HA1-S210 had earlier and higher peak titers in inoculated ferrets and was recovered at a higher frequency after airborne transmission than P4 and G15. Overall, a combination of enhanced polymerase activity and a stabilized HA protein promoted airborne transmission of swine H1N1 viruses in ferrets, and minor variants containing both properties were selected. The results suggest pandemic risk-assessment studies may benefit from deep sequencing to identify minor variants with human-adapted traits.

IMPORTANCE

Diverse IAVs circulate in avians, swine, and other species; however, few acquire the viral traits needed to start a human pandemic. A receptor-binding preference for α-2,6-linked sialic acid receptors is necessary but not sufficient for pandemic potential. Other viral traits are needed but are less well understood and are not explicitly considered in current pandemic risk-assessment algorithms. A stabilized HA and mammalian-adapted polymerase have been shown to promote the adaptation of IAVs to humans and ferrets (the gold-standard model for IAV replication, pathogenicity, and transmissibility). Here, we used swine IAV isolates of the gamma lineage as a model to investigate the importance of HA stability and polymerase activity in promoting replication and transmission in ferrets. These are emerging viruses that bind to both α-2,6- and α-2,3-linked receptors. Using isolates containing mixed populations, a stabilized HA was selected within days in inoculated ferrets. An enhanced polymerase was selected later in half of transmission events. Thus, HA stabilization was a stricter requirement, yet both traits promoted transmissibility in ferrets. Knowing the combination of viral traits needed for pandemic potential, and the relative importance of each, will help identify viruses of greatest concern.

INTRODUCTION

IAVs circulate in numerous species, and it remains challenging to identify animal-origin IAVs at greatest risk to cause a pandemic in humans. In addition to bats (1-3), IAVs originate from a reservoir of wild aquatic birds (4). From wild birds, avian IAVs can infect and either directly or indirectly become endemic in wild and domestic birds, swine, humans, and other domestic or aquatic mammals (5, 6). IAVs have eight RNA gene segments that encode for over a dozen proteins including an RNA-dependent RNA polymerase (RdRp) complex (PB1, PB2, and PA) and the surface glycoproteins hemagglutinin (HA) and neuraminidase (NA) (7, 8). Antigenically diverse HA and NA subtypes have been identified and currently number from H1-H18 and N1-N11. H1N1 caused the 1918 Spanish influenza pandemic, circulated in humans until 1957, became endemic in swine, reemerged in humans in 1977, and caused the 2009 pandemic (pH1N1) (8, 9). In 1957, H1N1 was supplanted in humans by the H2N2 Asian influenza pandemic. H2N2 was supplanted by the H3N2 Hong Kong influenza pandemic in 1968. H3N2 viruses, along with pH1N1 and influenza B viruses, cause seasonal influenza in humans. H1N1, H1N2, and H3N2 viruses are currently endemic in swine (10-12).

H1 swine viruses have been divided into six clades: alpha (1A.1), beta (1A.2), gamma (1A.3.3.3), H1pandemic (1A.3.3.2), delta1 (1B.2.2), and delta 2 (1B.2.1) (13, 14). Swine gamma and pandemic clades diverged approximately twenty years ago and have caused numerous human infections (15). Currently, H1 gamma clade is endemic in swine and frequently reassorts with human pandemic H1N1 isolates (16). Preparing for and responding to future human pandemics requires an understanding of viral traits and host markers associated with human adaptation so that high-risk emerging viruses can be identified, and countermeasures taken.

IAV adaptations that have been associated with human-to-human transmission include HA receptor-binding specificity, HA stability, polymerase complex efficiency, HA-NA balance,

NA stalk length, interferon antagonism, and filamentous virus morphology (5, 17). During viral entry, the HA protein binds sialic acid-containing receptors. This triggers virion endocytosis and acidification, which induces irreversible HA structural changes that cause membrane fusion. Human-adapted IAVs contain HA proteins that preferentially bind α-2,6-linked sialic acid (SA) receptors over α-2,3-linked ones, which are preferred by avian IAVs (8, 18-22). In human- and ferret-adapted IAVs, the avidity of the HA protein for cell-surface glycan receptors is balanced with the substrate selectivity and catalytic rate of the NA protein (17, 23-26). Decreased HA activation pH in the context of H5N1 viruses reduces replication and transmission in avian species but increases nasal replication and is required for airborne transmission in ferrets (27-34). Similarly, HA stabilization occurred during the adaptation of pH1N1 to humans (35, 36). HA stabilization has been shown to be necessary for airborne transmission of pH1N1 and swine H1N1 gamma viruses in ferrets, in part by increasing longevity of expelled virions (37-39).

The polymerases from avian IAVs are relatively inefficient at genome replication in mammalian cells (40, 41) Therefore, they require adaptative mutations in their polymerase complexes to replicate and transmit in mammals (42-44). Mammalian-adaptive PB2 mutations include T271A, G590S, Q591R, E627K, and D701N (5). PB2-E627K, the best-characterized mutation, was present in the 1918 H1N1, 1957 H2N2, and 1968 H3N2 pandemic viruses and has been associated with avian H7N9 and H5N1 influenza virus adaptation in humans and other mammalian hosts (45, 46). The 2009 pH1N1 virus lacked the PB2-E627K mutation but had phenotypically similar mutations PB2-G590S/Q591R, which were located near residue 627. The swine H1N1 gamma viruses in the present study have mammalian-preferred PB2-G590S/Q591R mutations and avian-like PB2-E627 and PB2-D701.

Influenza pandemic risk assessment algorithms by the US Centers for Disease Control and Prevention (CDC) and World Health Organization (WHO) explicitly consider HA receptor-

binding specificity and indirectly account for other human-adaptive viral traits through airborne transmission studies (47, 48). Ferrets are currently considered the gold-standard animal model to study transmission of influenza viruses (20, 49).

In a previous study, we found HA stabilization promoted the replication and transmission of swine H1N1 IAVs in ferrets (39). Related isolates A/swine/Illinois/2A-1213-G15/2013 (H1N1) and A/swine/Illinois/2B-0314-P4/2014 (H1N1) were found to have a single HA variation at residue 210 (H3 numbering) located between the receptor-binding domain heads, which resulted in HA activation pH values of 5.8 and 5.5, respectively. The G15 group had 3/3 airborne-transmission events in ferrets after selection of a stabilized variant (HA1-S210, HA activation pH 5.5). Despite also having an HA activation pH of 5.5, the P4 group had only 1/3 airborne transmission. The G15 and P4 viruses also contained polymerase gene variations at PB2-648 and PA-271, and P4 had minor variants at PA-321 and PA-386. Therefore, we hypothesized that P4 and G15 differed in polymerase activity in addition to HA stability and that enhanced polymerase activity contributed to increased airborne transmissibility of P4 over G15. Meanwhile, we could not rule out whether having an initial mixed population of HA stability in the case of P4 was responsible for increased airborne transmissibility. In the present work, we isolated the G15 virus containing the stabilizing HA1-S210 variation and studied replication and transmission of G15-HA1-S210, G15, and P4 viruses in ferrets. Overall, we found that both enhanced HA stability and polymerase activity are associated with airborne transmissibility in ferrets and that a mixed population of HA-stabilized and HA-destabilized fractions was not needed for replication and transmission in ferrets.

RESULTS

Impact of HA and polymerase variations on gamma virus replication in MDCK cells. Whole-genome sequencing analyses showed that five amino acid variations existed between swine H1N1 gamma viruses P4 and G15 (Fig. 1A). P4 contained 92% PA-N321, 8% PA-S321, 86% PA-D386, and 14% PA-N386, and we designated this virus isolate as P4-PA-mixed. We designated the G15 virus as G15-HA1-mixed because this virus isolate contained 85% HA1-N210 and 15% HA1-S210 (Fig. 1A). Aside from the minor variants, P4-PA-mixed and G15-HA1-mixed differed from each other at HA1-210, PA-271, and PB2-648 (Fig. 1A). From G15-HA1-mixed, we isolated the majority population (G15-HA1-N210) and the minor variant (G15-HA1-S210). Residue HA1-210 interacts with residues across the trimer interface in the head domain, so the HA1-S210 variation most likely stabilizes the HA protein by resisting dissociation of the heads (39).

After infection in Vero cells, the highest pH at which G15-HA1-mixed and G15-HA1-N210 were triggered to cause syncytium formation (cell-to-cell fusion) was 5.8 (Fig. 1B). P4-PA-mixed and G15-HA1-S210 had more stable HA proteins that were activated at pH 5.5 and 5.6, respectively. The pH of virus inactivation was measured by exposing virus aliquots to media of varying pH, neutralizing, and measuring residual infectivity. The pH at the midpoint of inactivation of G15-HA1-mixed and G15-HA1-N210 were 5.75 and 5.8, respectively, while those of P4-PA-mixed and G15-HA1-S210 were 5.6 (Fig. 1C). Overall, HA activation pH values were similar to virus inactivation values, G15-HA1-mixed and G15-HA1-N210 had relatively unstable HA proteins, and P4-PA-mixed and G15-HA1-S210 had stabilized HA proteins.

Previous reports showed differences in polymerase activity and/or HA stability may affect virus one-step growth (50-52). To explore this, we inoculated viruses into MDCK cells at an MOI of 2 PFU/cell and measured the virus titers of the supernatants at 6- and 8-hours post-

infection (hpi). Compared to P4-PA-mixed, the three other viruses had higher titers at 6 hpi (Fig. 1D). As P4-PA-mixed and G15-HA1-S210 have identical HA proteins, enhanced replication at 6 hpi was mapped to PA-P271 and/or PB2-L648. At 8 hpi, G15-HA-N210 had higher titers than the other three viruses. G15-HA1-N210 and G15-HA1-S210 were identical except for HA1 residue 210. Therefore, the HA1-N210 variation (HA activation pH 5.8) enhanced replication at 8 hpi in MDCK cells compared to HA1-S210 (pH 5.6). Overall, both the HA variation and the polymerase variations were found to modulate the production of infectious virus in MDCK cells at relatively early time points.

G15-HA1-S210 had higher polymerase activity than P4-PA-mixed. Virus polymerase activity can be assessed by the accumulation of viral mRNA, cRNA, and vRNA, which are produced in virus transcription and replication (53). To study the impact of the PB2 and PA variations on polymerase activity, we compared G15-HA1-S210 and P4-PA-mixed, which had identical HA genes. The viruses were inoculated into MDCK cells at an MOI of 2 PFU/cell and the resulting cell lysates and supernatants were harvested at 4 and 6 hpi. Compared to P4-PA-mixed, G15-HA1-S210 had higher mRNA, cRNA, and vRNA levels at 4 and 6 hpi (Fig. 2A-B). G15-HA1-S210 also had higher viral loads in cell supernatants at 6 hpi (Fig. 2C). Overall, the presence of PA-P271 and/or PB2-L648 in G15-HA1-S210 was associated with higher polymerase activity. These two variations were also present in G15-HA1-mixed and G15-HA1-N210.

Infection of donor ferrets inoculated with P4-PA-mixed, G15-HA1-mixed, and G15-HA1-S210. While G15-HA1-S210 had relatively efficient polymerase activity and a stabilized HA protein, P4-PA-mixed had decreased polymerase activity and G15-HA1-mixed had a relatively unstable HA protein (Fig. 3A). In each cubicle, three ferrets were directly inoculated with10^6 PFU of virus, and one day later we introduced three naïve contact and three naïve

airborne ferrets (Fig. 3B). Each virus group was evaluated in an isolated cubicle and personal protective equipment was changed before moving between cubicles to avoid cross contamination of viruses. Each cubicle was set to a temperature of approximately 22 °C and relative humidity 40-60 (Fig. S1). Here, we infected two cubicles of ferrets with G15-HA1-S210, so that this group had a total of n=18. We previously infected one cubicle of ferrets with P4-PA-mixed and G15-HA1-mixed each (n=9), which were the same as the present setting in Fig. 3B (39). We chose to continue to infect another cubicle of ferrets with P4-PA-mixed and G15-HA1-mixed each for the present study (n=9). Therefore, all three virus groups had a total of 18 ferrets (6 donor, 6 contact, and 6 airborne). All ferrets were monitored for body weight and temperature daily, and ferret nasal washes were collected every other day until day 14. Ferret sera were collected on day 21.

On day 1, G15-HA1-S210 donor ferrets had an average nasal wash titer of 2.18×10^7 $TCID_{50}$/ml, a value more than 10-fold higher than that of P4-PA-mixed (6.46×10^5 $TCID_{50}$/ml, $P = 0.039$) and 100-fold higher than G15-HA1-mixed (9.48×10^4 $TCID_{50}$/ml, $P = 0.0007$) (Fig. 3C and Table 1). G15-HA1-S210 had peak titers on day 1, while G15-HA1-mixed and P4-PA-mixed had mean peak titers on day 3 (Fig. 3D). Additionally, the average peak titer of G15-HA1-S210 in donor ferrets (2.18×10^7 $TCID_{50}$/ml) was significantly higher than that of G15-HA1-mixed (8.34×10^5 $TCID_{50}$/ml) (Fig. 3E). Overall, G15-HA1-S210, which had a stabilized HA and enhanced polymerase activity, had earlier and higher growth in the nasal cavities of inoculated ferrets.

The average HAI titers of donor ferret sera of G15-HA1-S210 were higher than those of P4-PA-mixed and G15-HA1-mixed (Fig. 3F). One donor ferret in cubicle 1 and two in cubicle 2 of G15-HA1-S210 had >10% body weight loss for at least two days, compared to no ferrets inoculated with P4-PA-mixed and G15-HA1-mixed ($P < 0.05$, Fig. 3G). No significant differences in body temperature were observed between the donor ferret groups (Fig. S2).

Contact and airborne transmission in P4-PA-mixed. P4-PA-mixed had 3/3 contact and 3/3 airborne transmission events (Fig. 4A and 4B). To determine if variants emerged during the experiment, we used next-generation sequencing to determine the whole genomes of viruses from ferret nasal washes. Single-nucleotide variants (SNVs) resulting in amino acid changes were observed for each sample. Minor variant PA-S321 represented approximately 8% of the inoculum (Fig. 1A and 4D). Interestingly, we found PA-S321 consistently appeared in donor, contact, and airborne ferrets with dominant percentages in the initial days of 2/3 airborne-transmitted ferret samples (Fig. 4C and 4D). Other PB1, HA, NP, and NS SNVs were detected in the first days of airborne transmitted samples in A1 and A2 ferrets. However, these variants did not enrich to higher percentages than PA-S321 and disappeared in both airborne-infected ferrets in the following days. We also detected other variants in PB2, HA, NP, and NS genes. However, these variants were either found only in a single ferret or were observed at low percentages. In our previous study, the P4 virus achieved 1/3 airborne transmission in ferrets without the selection of PA-S321 (39). Overall, minor variant PA-S321 played the most important role in airborne transmission and was associated with 2/4 airborne transmission events.

PA-S321 had enhanced polymerase activity. PA-N321S has been identified as an important human-adaptive mutation for avian H5 influenza A viruses (54, 55). Therefore, efficient airborne transmission in P4-PA-mixed was most likely due to propagation of the PA-S321 variant. We plaque purified P4-PA-S321 and compared this virus *in vitro* to P4-PA-mixed and G15-HA1-S210. P4-PA-S321 had higher levels of mRNA, cRNA, and vRNA at 4 and 6 hpi in MDCK cells than P4-PA-mixed, elevating polymerase activity to a level similar to G15-HA1-S210 (Fig. 5A-B). Compared to P4-PA-mixed, P4-PA-S321 also yielded higher virions released from MDCK cells at 6 hpi (Fig. 5C). P4-PA-S321 yielded RNA levels and virus titers similar to G15-HA1-S210 (Fig. 5A-C). Therefore, PA-S321 increased the polymerase activity to a level

similar to that of the G15 isolates, which had the alternative polymerase-enhancing variations PA-P271/PB2-L648.

Contact and airborne transmission of G15-HA1-mixed and G15-HA1-S210. The inoculum of G15-HA1-mixed contained approximately 15% HA1-S210 (Fig. 1A and 6D). HA1-S210 was present at a level greater than 90% in all donor ferrets within three days and was transmitted to all of the contact animals in the present study (Fig. 6 C-D). Thus, the stabilizing HA1-S210 variation was rapidly selected in inoculated ferrets and was exclusively transmitted. The inocula of the P4-PA-mixed and G15-HA1-S210 groups contained 100% HA1-S210, and this residue remained HA1-S210 during replication and transmission in ferrets (Fig. 4C and Fig. 8C). Therefore, all contact ferrets in G15-HA1-mixed, P4-PA-mixed, and G15-HA1-S210 contained the stabilizing HA1-S210 variation and had HA activation pH values of approximately 5.6 (Fig. 7A-D).

Airborne transmission of G15-HA1-mixed occurred in 2/3 ferrets, as detected by seroconversion (Fig. 6B). We were unable to isolate G15-HA1-mixed virus from the nasal washes of two seroconverted airborne ferrets in the present study (Fig. 6A). In our previous study (39), virus was recovered from 2/3 of airborne ferrets in the G15-HA1-mixed group and the recovered virus was exclusively G15-HA1-S210.

G15-HA1-S210 had a seroconversion rate of 4/6 after airborne transmission (Fig. 8A-B and Table 1). Airborne transmission occurred in 3/3 ferrets in cubicle one and 1/3 ferrets in cubicle two (Fig. 8A-B). The airborne ferret in cubicle two had early nasal virus growth on days 2-6, while all the other three airborne ferrets in cubicle one shed nasal virus between days 8 and 14 (Fig. 8A). G15-HA1-S210 also contained a variety of minor variants in the donor, contact, and airborne ferrets (Fig. 8C). PB1-E751STOP was the most-abundant variant in this group. However, PB1-E751STOP did not emerge on the initial day in airborne ferret A1, and it emerged

with a much lower percentage in ferret A3 in cubicle one (Fig. 8C). Additionally, we didn't detect this variant in the donor and contact ferrets. Therefore, this variant may not be associated with transmission. We re-cultured ferret nasal washes in MDCK cells and found more isolates growing successfully from the G15-HA1-S210 airborne group than from the airborne ferrets in the other two groups (Fig. 8D). There were no significant differences in body weight and temperature among the contact and airborne groups (Figs. S3 and S4).

In summary, the G15-HA1-mixed inoculum contained 15% HA1-S210 and this HA-stabilized variant was selected within inoculated ferrets within days and was exclusively transmitted by contact and airborne routes. For all groups studied, all airborne-transmitted viruses had HA activation pH values of 5.5-5.6 and none retained an HA activation pH of 5.8 (Fig. 9). The P4-PA-mixed inoculum contained 8% PA-S321, this polymerase-enhancing variant remained as a minor population in donor and contact ferrets, and PA-S321 was detected in 2/4 airborne ferrets. Thus, for all groups studied, 11/13 viruses in the airborne ferrets had the polymerase-enhancing variation while 2/13 retained lower polymerase activity (Fig. 9). Overall, a stabilized HA protein was more stringently selected than enhanced polymerase activity, yet both a stable HA and an efficient polymerase were associated with airborne transmission.

DISCUSSION

Three viral traits thought to be necessary for human-to-human and ferret-to-ferret transmissibility by influenza A viruses are HA receptor-binding specificity for α-2,6-linked sialic-acid receptors, an HA protein relatively resistant to acid-induced activation/inactivation, and a polymerase complex capable of efficient replication in mammalian cells (5, 17). The swine H1N1 gamma viruses studied here have been shown to bind α-2,6-linked receptors with high affinity in addition to having lower-level binding to α-2,3-linked receptors (39). P4-PA-mixed had a stabilized HA protein but lacked an efficient polymerase, and G15-HA1-mixed had an efficient polymerase but a relatively unstable HA protein. Both virus isolates contained minority variants at a level of 8-15% abundance that overcame the respective deficiency. These variants were selected in ferrets and accounted for 2/3 of P4-PA-mixed and all of G15-HA1-mixed airborne transmission events. Compared to P4-PA-mixed and G15-HA1-mixed, variant G15-HA1-S210, which contained both a stabilized HA protein and an efficient polymerase, had increased early growth in the nasal cavities of inoculated ferrets and was recovered in greater abundance from the nasal cavities of airborne-exposed ferrets. Overall, the data demonstrated that the combination of HA stability and polymerase efficiency promotes efficient airborne transmissibility of swine H1N1 gamma viruses in ferrets and that minor variants containing both traits can be selected and airborne transmitted when the majority of a virus sample lacks a stabilized HA or an efficient polymerase.

Multiple traits are required for IAV airborne transmissibility in ferrets, and it is important to understand if these traits must be acquired in a particular order or if they may evolve in any order. For IAVs already possessing α-2,6 receptor-binding specificity, the present study revealed two evolutionary pathways for the enhancement of ferret airborne transmissibility: (A) from a virus quasispecies that has an efficient polymerase, a minor variant with a stabilized HA protein

may be selected, or (B) from a virus quasispecies with a stabilized HA protein, a minor variant with an enhanced polymerase may be selected.

With respect to pathway A, several other studies showed that an IAV containing α-2,6 receptor-binding specificity and an efficient polymerase, but having a relatively unstable HA protein, can acquire airborne transmissibility in ferrets by acquiring an HA-stabilizing mutation. Wild-type 2009 pH1N1 has an HA activation pH of 5.5, and a destabilizing HA1-Y17H mutation increased this value to 6.0 (37, 52, 56). The HA1-Y17H mutant was attenuated in ferrets and did not airborne transmit until acquiring stabilizing HA2-R106K and HA1-H17Y mutations, which decreased the HA activation pH to 5.3 (37). Mechanistically, HA stabilization was shown to increase replication in human airway cells (57), dampen Type I interferon responses in dendritic cells (52), and increase the survivability of infectious virions after respiratory expulsion in ferrets (38). In another study, a recombinant virus was generated that contained the HA from A/Vietnam/1203/2004 (H5N1) with two HA mutations that conferred α2,6 receptor-binding specificity, and the other seven genes from A/California/04/2009 (H1N1) with a PB2-E627K mutation that enhanced polymerase activity (27). This virus and an adaptive mutant containing an HA1-N158D mutation that deleted a glycosylation on the HA head were incapable of airborne transmissibility in ferrets. Instead, a final mutation needed for the acquisition of airborne transmissibility was HA1-T318I in the stalk, which decreased the HA activation pH to 5.3. When HA-stabilizing mutations were introduced into other H5N1 viruses lacking α2,6 receptor-binding specificity, virus growth in the nasal cavities of ferrets was enhanced but airborne transmission did not occur (29, 30, 58).

With respect to pathway B, P4-PA-mixed had a stabilized HA protein and its airborne transmission in 2/4 cases was associated with selection of the PA-S321 mutation that enhanced polymerase activity. A/Indonesia/5/2005 (H5N1) acquired airborne transmissibility in ferrets by

a combination of mutagenesis and adaptation that enhanced receptor-binding activity (HA-T156A and HA-Q222L or HA-G224S), polymerase activity (PB2-E627K and PB1-H99Y), and HA stability (HA-H103Y) (28, 59). These mutations arose at similar steps during adaptation, and viruses lacking any of the single mutations HA-T156A, PB2-E627K, PB1-H99Y, or HA-H103Y, or both the HA-Q222L or HA-G224S mutations, were loss-of-function for airborne transmission in ferrets. In the case of reassortant IAVs containing genes from the human 1918 virus and avian H1N1 viruses, the human HA gene enabled efficient contact transmission but did not allow airborne transmission in ferrets (20). Instead, the human 1918 PB2 protein was found to be both necessary and sufficient to enable ferret airborne transmission in the context of a virus that contained the human 1918 HA and NA genes. Thus, while selection of enhanced polymerase activity in the present work was less stringent than selection of a stabilized HA, the adaptation of IAVs for airborne transmission in ferrets, and presumably in humans, has been associated with both HA stability and polymerase activity and both pathways A and B appear viable.

Quasispecies have been associated with IAV fitness and virulence in various hosts (60, 61). In this study, minor variants of swine H1N1 viruses with enhanced polymerase activity or HA stability were selected in ferrets and associated with airborne transmissibility. The transmission of minor variants has been previously observed for IAVs in humans (62), equines (63), and guinea pigs (64). This suggests minor variants, in addition to the majority population of a virus, need to be considered when assessing the risk of IAVs for human pandemic potential. Next-generation sequencing has been used to track the outgrowth of HA-stabilizing variants in ferrets in this study and others (37-39, 56). Deep sequencing of samples from H7N9-infected patients and their surrounding poultry/environment showed acquisition of the polymerase-enhancing PB2-E627K variation in humans (45). H3N2 and H1N1 growth in mice has been shown to not necessarily proceed through linear accumulation of adaptative mutations (65).

Overall, as next-generation sequencing becomes cheaper, faster, and more efficient, real-time monitoring of human-adaptive variations may enable better preparedness for future outbreaks.

Numerous studies have been performed to identify and characterize human- and ferret-adaptive mutations in IAVs. Examples include those focusing on the polymerase complex (42, 51, 66-72) and the HA protein (38, 56, 58, 73-81) In the present study, we found G15 isolates containing PB2-L648/PA-P271 had higher polymerase activities than P4-PA-mixed, which contained PB2-M648/PA-T271. PB2-L648 was previously shown to increase polymerase activity of an H10N8 virus (82). The present study also showed that PA-S321 increased polymerase activity. PA-S321 has previously been identified as an adaptative marker for H5N1 influenza A viruses in humans (54, 55, 83). The HA1-S210 mutation was shown to decrease the pH of HA activation and the pH of virus inactivation here and in our previous work (39).

In summary, a combination of efficient polymerase activity and a stabilized HA were found to enhance airborne transmission of swine H1N1 gamma viruses in ferrets, and these two properties may be acquired in either order. Human infections of seasonal influenza viruses have been far less frequent since the start of the SARS-CoV-2 pandemic, mask mandates, and social distancing. Widespread reemergence of seasonal influenza is expected to occur in the post-SARS-CoV-2-pandemic era. Ultimately, exotic IAVs in other species, especially swine, and the potential for cross-species transmission make it essential to monitor potential pandemic IAV strains and to assess their pandemic risk. Swine H1N1 gamma viruses are one of the most prevalent lineages in swine (84), have caused sporadic human infections in recent years (15, 85), and have been shown here to acquire increased transmissibility in ferrets by adaptive HA and polymerase mutations. A recent study has identified a swine Eurasian avian-like influenza virus with pandemic traits (86). Surveillance and risk assessment studies are needed for IAV pandemic

preparedness in addition to studies investigating the evolutionary pathways by which pandemic potential may arise and genetic and phenotypic traits associated therewith.

MATERIALS AND METHODS

Cells and viruses

Madin–Darby canine kidney (MDCK) cells were maintained in minimum essential medium (MEM, Thermo Fisher Scientific). African green monkey kidney (Vero) cells were maintained in Dulbecco's Modified Eagle Medium (DMEM, Life Technologies™). Both culture media were supplemented with 10% HyClone® standard fetal bovine serum (FBS, Life Technologies) and 1% penicillin/streptomycin (P/S, Thermo Fisher Scientific). The cells were grown at 37 °C with 5% CO_2 (50, 51).

A/swine/Illinois/2A-1213-G15/2013 (H1N1) (G15-HA1-mixed) and A/swine/Illinois/2B-0314-P4/2014 (H1N1) (P4-PA-mixed) were originally isolated from nasal swabs from pigs in commercial swine herds in the United States that showed symptoms of influenza-like illness, as described previously (39, 87). G15-HA1-S210 and G15-HA1-N210 were plaque purified twice from MDCK cells using G15-HA1-mixed. The whole-genome sequences of G15-HA1-S210 and G15-HA1-N210 were verified by next-generation sequencing. All viruses were propagated in MDCK cells with 1 μg/ml tosylsulfonyl phenylalanyl chloromethyl ketone (TPCK)–treated trypsin, as described previously (39, 50).

Syncytium assay

Viruses were inoculated into Vero cells in 24–well plates at a multiplicity (MOI) of 3 PFU/cell. After maintaining at 37 °C with 5% CO_2 for 16 hours (h), the infected cells were treated with DMEM supplemented with 5 μg/ml TPCK–treated trypsin for 15 minutes (m) and then pH–adjusted PBS buffers for 15 m. Subsequently, the infected cells were maintained in DMEM supplemented with 5% FBS for 3 h at 37 °C. After that, the infected cells were fixed and stained using a Hema 3™ Fixative and Solutions (Fisher Scientific). Syncytia were recorded using a light microscope. The cutoff values for virus HA activation pH were determined at the

treated pH that the stained cells in 24-well plates containing more than two syncytia with at least five nuclei, as described previously (39, 52, 88).

HA inactivation pH assay

Tested viruses were treated with a series of pH-adjusted PBS buffers in a ratio of 1:100 for 1 h at 37 °C. The resulting infectious viruses were titrated by $TCID_{50}$ on MDCK cells (30, 37). After obtaining virus titers for treatments, HA inactivation pH values were calculated by using GraphPad Prism version 7 software (Graph-Pad Software, San Diego, CA). The parameter LogEC50 was generated using the model Nonlinear Regression [Equation: log (agonist) vs. response-Variable slope (four parameters)] followed by the least squares fitting method.

Virus growth assay

Tested viruses were inoculated into MDCK cells in 24–well plates at an MOI of 2 PFU/cell. After incubation for 1 h at 37 ºC, the infected cells were washed by PBS twice, and continued to be maintained at 37 ºC with MEM culture media (1 ml/well) supplemented with 1 µg/ml TPCK-treated trypsin. At 6- and 8-hours post-infection (hpi), cell culture supernatant was collected and titrated by $TCID_{50}$ on MDCK cells (37, 89).

Virus mRNA, cRNA and vRNA quantification

Production of virus RNAs (mRNA, cRNA, and vRNA) during influenza A virus transcription and replication processes were quantified using a two-step real time RT-qPCR, modified from the method described previously (51, 68, 90). Briefly, viruses were inoculated into confluent MDCK cells in 24–well plates at an MOI of 2. The infected cells were incubated at 37 °C for 1 h, washed by PBS twice, and cultured with MEM supplemented with 1 ug/ml TPCK-treated trypsin (1 ml/well). At 4 and 6 hpi, culture supernatants and infected cells were harvested separately.

To quantify virus mRNA, cRNA, and vRNA, total RNAs were extracted from the infected cells using RNeasy Mini Kit (Qiagen). The corresponding cDNAs of mRNA, cRNA, and vRNA were generated by reverse-transcription PCR (RT-PCR) using Transcriptor First Strand cDNA Synthesis Kit (Roche). Primers with specific tags for differentiations of virus mRNA, cRNA, and RNA were used (mRNA-RT-PCR primer: CCAGATCGTTCGAGTCGTTTTTTTTTTTTTTTTTCTCATGTTTCT; cRNA-RT-PCR primer: GCTAGCTTCAGCTAGGCATCAGTAGAAACAAGGGTGTTTTTTCTC; vRNA-RT-PCR primer: GGCCGTCATGGTGGCGAATTGGCCACAGGATTAAGGAATATC)

Real-time quantitation PCR were performed to quantify these three RNA levels with specific primers targeting virus HA gene (mRNA-real time-forward primer (FP): CCAGTTCATTGGTACTGGTAGTC, mRNA-real time-reverse primer (RP): CCAGATCGTTCGAGTCGT; cRNA-real time-FP: CCAGTTCATTGGTACTGGTAGTC, cRNA-real time-RP: GCTAGCTTCAGCTAGGCATC; vRNA-real time-FP: GGCCGTCATGGTGGCGAAT, vRNA-real time-RP: ACCGTACCACCCATCTATCA;). Internal control GAPDH mRNA was also reverse-transcribed and quantified using oligo $(dT)_{20}$ as RT-PCR primer and the following as real-time PCR primers (FP: ATTCCACCCATGGCAAATTC, RP: CGCTCCTGGAAGATGGTGAT).

To quantify viral copy number released in cell-free supernatant, total RNAs were extracted using QIAamp Viral RNA kits (Qiagen). A two-step quantitative real-time reverse-transcription (RT) PCR was applied to quantify viral copy number. The primers used were listed as the following, RT-PCR-primer: AGCAAAAGCAGG; Real-time-FP (targeting NP gene): CTGCTTGTGTGTATGGGCTT; Real-time-RP (targeting NP gene): TGAGCTGGATTTTCATTTGGT. Plasmid PHW2000-NP (G15-HA1-mixed) was used as a standard for quantitative real-time PCR.

Ferret transmission experiments

Thirty-six male Fitch ferrets (five- to six-month-old, purchased from Triple F Farms, Sayre, PA) were verified to be serologically negative for currently circulating influenza A and B viruses and the tested swine H1N1 gamma influenza viruses by HAI assay. At the same time, these ferrets were identified to be serologically negative for currently circulating SARS-CoV-2 by ELISA. The nasal swabs of these ferrets were verified to be negative before the experiments by performing real-time PCR reactions.

The transmission study was performed as described in previous work (39). Ferret body weight and temperature were monitored daily until day 14. Ferret nasal washes were collected every other day until day 14. Additionally, all ferrets were euthanized on day 21 to collect whole blood. Ferret sera were examined for seroconversion using HAI assay (37, 39, 88). Animal studies were performed in compliance with St. Jude Children's Research Hospital Animal Care and Use Committee guidelines under protocol 459.

Virus whole-genome sequencing and analyses

Virus whole genomes were obtained by next-generation sequencing (39, 56, 88). Viral RNAs were extracted from ferret nasal wash samples or cell-free supernatants using QIAamp Viral RNA kits (Qiagen). The corresponding cDNAs were achieved by reverse–transcription PCR using SuperScript III First-strand Synthesis System (Thermo Fisher Scientific). DNA library was prepared by PCR amplification using Phusion High-Fidelity PCR Master Mix with HF Buffer (New England BioLabs). The resulting PCR products were purified by QIAquick Gel Extraction Kit (Qiagen) and submitted to St Jude Harwell Center for virus whole-genome sequencing.

Sequencing data were analyzed using CLC Genomics Workbench version 11.0.1. SNVs resulting amino-acid variations were reported when the predefined quality scores were met and

present in forward and reverse reads at an equal ratio. All variants presented in this study were supported by at least 10 reads with a minimum frequency of 5% (unless otherwise stated). Heat maps and parts of whole were generated by using GraphPad Prism version 7 software (GraphPad Software, San Diego, CA).

Statistical analysis

All data analyses were performed using GraphPad Prism version 7. One-way ANOVA followed by a Tukey's multiple comparisons test, Welch's *t* test or Mann-Whitney U test were used to determine statistical significances. P value < 0.05 was considered significant.

ACKNOWLEDGMENTS

We thank Guohua Yang, Ashley Webb, and Melissa Penaflor for help with ferret experiments. We also thank St. Jude Animal Resources Center for help with ferret experiments. We thank the Hartwell Center DNA Sequencing & Genotyping, Hartwell Center Functional Genomics, and the Hartwell Center Genome Sequencing Facility. This work was funded, in part, by the National Institute of Allergy and Infectious Diseases under Centers of Excellence for Influenza Research and Surveillance (CEIRS) contract no. HHSN272201400006C, St. Jude Children's Research Hospital, and the American Lebanese Syrian Associated Charities (ALSAC). The content is solely the responsibility of the authors and does not necessarily represent the official views of the National Institutes of Health.

CONFLICT OF INTEREST

The authors declare no competing financial interests.

References

1. Tong S, Li Y, Rivailler P, Conrardy C, Castillo DA, Chen LM, Recuenco S, Ellison JA, Davis CT, York IA, Turmelle AS, Moran D, Rogers S, Shi M, Tao Y, Weil MR, Tang K, Rowe LA, Sammons S, Xu X, Frace M, Lindblade KA, Cox NJ, Anderson LJ, Rupprecht CE, Donis RO. 2012. A distinct lineage of influenza A virus from bats. Proc Natl Acad Sci U S A 109:4269-74.
2. Tong S, Zhu X, Li Y, Shi M, Zhang J, Bourgeois M, Yang H, Chen X, Recuenco S, Gomez J, Chen LM, Johnson A, Tao Y, Dreyfus C, Yu W, McBride R, Carney PJ, Gilbert AT, Chang J, Guo Z, Davis CT, Paulson JC, Stevens J, Rupprecht CE, Holmes EC, Wilson IA, Donis RO. 2013. New world bats harbor diverse influenza A viruses. PLoS Pathog 9:e1003657.
3. Kandeil A, Gomaa MR, Shehata MM, El Taweel AN, Mahmoud SH, Bagato O, Moatasim Y, Kutkat O, Kayed AS, Dawson P, Qiu X, Bahl J, Webby RJ, Karesh WB, Kayali G, Ali MA. 2018. Isolation and characterization of a distinct influenza A virus from Egyptian bats. J Virol doi:10.1128/JVI.01059-18.
4. Webster RG, Bean WJ, Gorman OT, Chambers TM, Kawaoka Y. 1992. Evolution and ecology of influenza A viruses. Microbiol Rev 56:152-79.
5. Long JS, Mistry B, Haslam SM, Barclay WS. 2019. Host and viral determinants of influenza A virus species specificity. Nat Rev Microbiol 17:67-81.
6. Russell CJ, Hu M, Okda FA. 2018. Influenza Hemagglutinin Protein Stability, Activation, and Pandemic Risk. Trends Microbiol doi:10.1016/j.tim.2018.03.005.
7. Shi Y, Wu Y, Zhang W, Qi J, Gao GF. 2014. Enabling the 'host jump': structural determinants of receptor-binding specificity in influenza A viruses. Nat Rev Microbiol 12:822-31.

8. Schrauwen EJ, Fouchier RA. 2014. Host adaptation and transmission of influenza A viruses in mammals. Emerg Microbes Infect 3:e9.

9. Webster RG, Govorkova EA. 2014. Continuing challenges in influenza. Ann N Y Acad Sci 1323:115-39.

10. Webby RJ, Rossow K, Erickson G, Sims Y, Webster R. 2004. Multiple lineages of antigenically and genetically diverse influenza A virus co-circulate in the United States swine population. Virus Res 103:67-73.

11. Gao S, Anderson TK, Walia RR, Dorman KS, Janas-Martindale A, Vincent AL. 2017. The genomic evolution of H1 influenza A viruses from swine detected in the United States between 2009 and 2016. J Gen Virol 98:2001-2010.

12. Walia RR, Anderson TK, Vincent AL. 2019. Regional patterns of genetic diversity in swine influenza A viruses in the United States from 2010 to 2016. Influenza Other Respir Viruses 13:262-273.

13. Anderson TK, Nelson MI, Kitikoon P, Swenson SL, Korslund JA, Vincent AL. 2013. Population dynamics of cocirculating swine influenza A viruses in the United States from 2009 to 2012. Influenza Other Respir Viruses 7 Suppl 4:42-51.

14. Anderson TK, Macken CA, Lewis NS, Scheuermann RH, Van Reeth K, Brown IH, Swenson SL, Simon G, Saito T, Berhane Y, Ciacci-Zanella J, Pereda A, Davis CT, Donis RO, Webby RJ, Vincent AL. 2016. A Phylogeny-Based Global Nomenclature System and Automated Annotation Tool for H1 Hemagglutinin Genes from Swine Influenza A Viruses. mSphere 1.

15. Pulit-Penaloza JA, Belser JA, Tumpey TM, Maines TR. 2019. Sowing the Seeds of a Pandemic? Mammalian Pathogenicity and Transmissibility of H1 Variant Influenza Viruses from the Swine Reservoir. Trop Med Infect Dis 4.

16. Ducatez MF, Hause B, Stigger-Rosser E, Darnell D, Corzo C, Juleen K, Simonson R, Brockwell-Staats C, Rubrum A, Wang D, Webb A, Crumpton JC, Lowe J, Gramer M, Webby RJ. 2011. Multiple reassortment between pandemic (H1N1) 2009 and endemic influenza viruses in pigs, United States. Emerg Infect Dis 17:1624-9.

17. Lipsitch M, Barclay W, Raman R, Russell CJ, Belser JA, Cobey S, Kasson PM, Lloyd-Smith JO, Maurer-Stroh S, Riley S, Beauchemin CA, Bedford T, Friedrich TC, Handel A, Herfst S, Murcia PR, Roche B, Wilke CO, Russell CA. 2016. Viral factors in influenza pandemic risk assessment. Elife 5.

18. Russell RJ, Stevens DJ, Haire LF, Gamblin SJ, Skehel JJ. 2006. Avian and human receptor binding by hemagglutinins of influenza A viruses. Glycoconj J 23:85-92.

19. Rajao DS, Anderson TK, Kitikoon P, Stratton J, Lewis NS, Vincent AL. 2018. Antigenic and genetic evolution of contemporary swine H1 influenza viruses in the United States. Virology 518:45-54.

20. Van Hoeven N, Pappas C, Belser JA, Maines TR, Zeng H, Garcia-Sastre A, Sasisekharan R, Katz JM, Tumpey TM. 2009. Human HA and polymerase subunit PB2 proteins confer transmission of an avian influenza virus through the air. Proc Natl Acad Sci U S A 106:3366-71.

21. Peacock TP, Sealy JE, Harvey WT, Benton DJ, Reeve R, Iqbal M. 2020. Genetic determinants of receptor-binding preference and zoonotic potential of H9N2 avian influenza viruses. J Virol doi:10.1128/JVI.01651-20.

22. Herfst S, Zhang J, Richard M, McBride R, Lexmond P, Bestebroer TM, Spronken MIJ, de Meulder D, van den Brand JM, Rosu ME, Martin SR, Gamblin SJ, Xiong X, Peng W, Bodewes R, van der Vries E, Osterhaus A, Paulson JC, Skehel JJ, Fouchier RAM. 2020.

Hemagglutinin Traits Determine Transmission of Avian A/H10N7 Influenza Virus between Mammals. Cell Host Microbe 28:602-613 e7.

23. Zanin M, Marathe B, Wong SS, Yoon SW, Collin E, Oshansky C, Jones J, Hause B, Webby R. 2015. Pandemic Swine H1N1 Influenza Viruses with Almost Undetectable Neuraminidase Activity Are Not Transmitted via Aerosols in Ferrets and Are Inhibited by Human Mucus but Not Swine Mucus. J Virol 89:5935-48.

24. Baum LG, Paulson JC. 1991. The N2 neuraminidase of human influenza virus has acquired a substrate specificity complementary to the hemagglutinin receptor specificity. Virology 180:10-5.

25. Yen HL, Liang CH, Wu CY, Forrest HL, Ferguson A, Choy KT, Jones J, Wong DD, Cheung PP, Hsu CH, Li OT, Yuen KM, Chan RW, Poon LL, Chan MC, Nicholls JM, Krauss S, Wong CH, Guan Y, Webster RG, Webby RJ, Peiris M. 2011. Hemagglutinin-neuraminidase balance confers respiratory-droplet transmissibility of the pandemic H1N1 influenza virus in ferrets. Proc Natl Acad Sci U S A 108:14264-9.

26. Handel A, Akin V, Pilyugin SS, Zarnitsyna V, Antia R. 2014. How sticky should a virus be? The impact of virus binding and release on transmission fitness using influenza as an example. J R Soc Interface 11:20131083.

27. Imai M, Watanabe T, Hatta M, Das SC, Ozawa M, Shinya K, Zhong G, Hanson A, Katsura H, Watanabe S, Li C, Kawakami E, Yamada S, Kiso M, Suzuki Y, Maher EA, Neumann G, Kawaoka Y. 2012. Experimental adaptation of an influenza H5 HA confers respiratory droplet transmission to a reassortant H5 HA/H1N1 virus in ferrets. Nature 486:420-8.

28. Herfst S, Schrauwen EJ, Linster M, Chutinimitkul S, de Wit E, Munster VJ, Sorrell EM, Bestebroer TM, Burke DF, Smith DJ, Rimmelzwaan GF, Osterhaus AD, Fouchier RA.

2012. Airborne transmission of influenza A/H5N1 virus between ferrets. Science 336:1534-41.

29. Shelton H, Roberts KL, Molesti E, Temperton N, Barclay WS. 2013. Mutations in haemagglutinin that affect receptor binding and pH stability increase replication of a PR8 influenza virus with H5 HA in the upper respiratory tract of ferrets and may contribute to transmissibility. J Gen Virol 94:1220-9.

30. Zaraket H, Bridges OA, Duan S, Baranovich T, Yoon SW, Reed ML, Salomon R, Webby RJ, Webster RG, Russell CJ. 2013. Increased acid stability of the hemagglutinin protein enhances H5N1 influenza virus growth in the upper respiratory tract but is insufficient for transmission in ferrets. J Virol 87:9911-22.

31. Reed ML, Bridges OA, Seiler P, Kim JK, Yen HL, Salomon R, Govorkova EA, Webster RG, Russell CJ. 2010. The pH of activation of the hemagglutinin protein regulates H5N1 influenza virus pathogenicity and transmissibility in ducks. J Virol 84:1527-35.

32. Richard M, Herfst S, van den Brand JMA, de Meulder D, Lexmond P, Bestebroer TM, Fouchier RAM. 2017. Mutations Driving Airborne Transmission of A/H5N1 Virus in Mammals Cause Substantial Attenuation in Chickens only when combined. Sci Rep 7:7187.

33. Russell CJ. 2014. Acid-induced membrane fusion by the hemagglutinin protein and its role in influenza virus biology. Curr Top Microbiol Immunol 385:93-116.

34. Russell CJ. 2021. Hemagglutinin Stability and Its Impact on Influenza A Virus Infectivity, Pathogenicity, and Transmissibility in Avians, Mice, Swine, Seals, Ferrets, and Humans. Viruses 13.

35. Maurer-Stroh S, Lee RT, Eisenhaber F, Cui L, Phuah SP, Lin RT. 2010. A new common mutation in the hemagglutinin of the 2009 (H1N1) influenza A virus. PLoS Curr 2:RRN1162.

36. Klein EY, Blumenkrantz D, Serohijos A, Shakhnovich E, Choi JM, Rodrigues JV, Smith BD, Lane AP, Feldman A, Pekosz A. 2018. Stability of the Influenza Virus Hemagglutinin Protein Correlates with Evolutionary Dynamics. mSphere 3.

37. Russier M, Yang G, Rehg JE, Wong SS, Mostafa HH, Fabrizio TP, Barman S, Krauss S, Webster RG, Webby RJ, Russell CJ. 2016. Molecular requirements for a pandemic influenza virus: An acid-stable hemagglutinin protein. Proc Natl Acad Sci U S A 113:1636-41.

38. Singanayagam A, Zhou J, Elderfield RA, Frise R, Ashcroft J, Galiano M, Miah S, Nicolaou L, Barclay WS. 2020. Characterising viable virus from air exhaled by H1N1 influenza-infected ferrets reveals the importance of haemagglutinin stability for airborne infectivity. PLoS Pathog 16:e1008362.

39. Hu M, Yang G, DeBeauchamp J, Crumpton JC, Kim H, Li L, Wan XF, Kercher L, Bowman AS, Webster RG, Webby RJ, Russell CJ. 2020. HA stabilization promotes replication and transmission of swine H1N1 gamma influenza viruses in ferrets. Elife 9.

40. Manz B, Brunotte L, Reuther P, Schwemmle M. 2012. Adaptive mutations in NEP compensate for defective H5N1 RNA replication in cultured human cells. Nat Commun 3:802.

41. Cauldwell AV, Long JS, Moncorge O, Barclay WS. 2014. Viral determinants of influenza A virus host range. J Gen Virol 95:1193-1210.

42. Mehle A, Doudna JA. 2009. Adaptive strategies of the influenza virus polymerase for replication in humans. Proc Natl Acad Sci U S A 106:21312-6.

43. Gabriel G, Klingel K, Otte A, Thiele S, Hudjetz B, Arman-Kalcek G, Sauter M, Shmidt T, Rother F, Baumgarte S, Keiner B, Hartmann E, Bader M, Brownlee GG, Fodor E, Klenk HD. 2011. Differential use of importin-alpha isoforms governs cell tropism and host adaptation of influenza virus. Nat Commun 2:156.

44. Gabriel G, Fodor E. 2014. Molecular determinants of pathogenicity in the polymerase complex. Curr Top Microbiol Immunol 385:35-60.

45. Liu WJ, Li J, Zou R, Pan J, Jin T, Li L, Liu P, Zhao Y, Yu X, Wang H, Liu G, Jiang H, Bi Y, Liu L, Yuen KY, Liu Y, Gao GF. 2020. Dynamic PB2-E627K substitution of influenza H7N9 virus indicates the in vivo genetic tuning and rapid host adaptation. Proc Natl Acad Sci U S A 117:23807-23814.

46. Hatta M, Gao P, Halfmann P, Kawaoka Y. 2001. Molecular basis for high virulence of Hong Kong H5N1 influenza A viruses. Science 293:1840-2.

47. Centers for Disease Control and Prevention. 2019, posting date. Influenza Risk Assessment Tool (IRAT). https://www.cdc.gov/flu/pandemic-resources/national-strategy/risk-assessment.htm.

48. World Health Organization. 2020, posting date. Tool for Influenza Pandemic Risk Assessment (TIPRA). https://www.who.int/publications/m/item/tool-for-influenza-pandemic-risk-assessment-(tipra).

49. Belser JA, Eckert AM, Huynh T, Gary JM, Ritter JM, Tumpey TM, Maines TR. 2020. A Guide for the Use of the Ferret Model for Influenza Virus Infection. Am J Pathol 190:11-24.

50. Hu M, Chu H, Zhang K, Singh K, Li C, Yuan S, Chow BK, Song W, Zhou J, Zheng BJ. 2016. Amino acid substitutions V63I or A37S/I61T/V63I/V100A in the PA N-terminal domain increase the virulence of H7N7 influenza A virus. Sci Rep 6:37800.

51. Hu M, Yuan S, Zhang K, Singh K, Ma Q, Zhou J, Chu H, Zheng BJ. 2017. PB2 substitutions V598T/I increase the virulence of H7N9 influenza A virus in mammals. Virology 501:92-101.

52. Russier M, Yang G, Briard B, Meliopoulos V, Cherry S, Kanneganti TD, Schultz-Cherry S, Vogel P, Russell CJ. 2020. Hemagglutinin Stability Regulates H1N1 Influenza Virus Replication and Pathogenicity in Mice by Modulating Type I Interferon Responses in Dendritic Cells. J Virol 94.

53. Te Velthuis AJW, Long JS, Barclay WS. 2018. Assays to Measure the Activity of Influenza Virus Polymerase. Methods Mol Biol 1836:343-374.

54. Miotto O, Heiny AT, Albrecht R, Garcia-Sastre A, Tan TW, August JT, Brusic V. 2010. Complete-proteome mapping of human influenza A adaptive mutations: implications for human transmissibility of zoonotic strains. PLoS One 5:e9025.

55. El-Shesheny R, Kandeil A, Bagato O, Maatouq AM, Moatasim Y, Rubrum A, Song MS, Webby RJ, Ali MA, Kayali G. 2014. Molecular characterization of avian influenza H5N1 virus in Egypt and the emergence of a novel endemic subclade. J Gen Virol 95:1444-1463.

56. Russier M, Yang G, Marinova-Petkova A, Vogel P, Kaplan BS, Webby RJ, Russell CJ. 2017. H1N1 influenza viruses varying widely in hemagglutinin stability transmit efficiently from swine to swine and to ferrets. PLoS Pathog 13:e1006276.

57. Singanayagam A, Zambon M, Barclay WS. 2019. Influenza Virus with Increased pH of Hemagglutinin Activation Has Improved Replication in Cell Culture but at the Cost of Infectivity in Human Airway Epithelium. J Virol 93.

58. Zaraket H, Bridges OA, Russell CJ. 2013. The pH of activation of the hemagglutinin protein regulates H5N1 influenza virus replication and pathogenesis in mice. J Virol 87:4826-34.

59. Linster M, van Boheemen S, de Graaf M, Schrauwen EJA, Lexmond P, Manz B, Bestebroer TM, Baumann J, van Riel D, Rimmelzwaan GF, Osterhaus A, Matrosovich M, Fouchier RAM, Herfst S. 2014. Identification, characterization, and natural selection of mutations driving airborne transmission of A/H5N1 virus. Cell 157:329-339.

60. Lauring AS, Andino R. 2010. Quasispecies theory and the behavior of RNA viruses. PLoS Pathog 6:e1001005.

61. Honce R, Karlsson EA, Wohlgemuth N, Estrada LD, Meliopoulos VA, Yao J, Schultz-Cherry S. 2020. Obesity-Related Microenvironment Promotes Emergence of Virulent Influenza Virus Strains. mBio 11.

62. Poon LL, Song T, Rosenfeld R, Lin X, Rogers MB, Zhou B, Sebra R, Halpin RA, Guan Y, Twaddle A, DePasse JV, Stockwell TB, Wentworth DE, Holmes EC, Greenbaum B, Peiris JS, Cowling BJ, Ghedin E. 2016. Quantifying influenza virus diversity and transmission in humans. Nat Genet 48:195-200.

63. Hughes J, Allen RC, Baguelin M, Hampson K, Baillie GJ, Elton D, Newton JR, Kellam P, Wood JL, Holmes EC, Murcia PR. 2012. Transmission of equine influenza virus during an outbreak is characterized by frequent mixed infections and loose transmission bottlenecks. PLoS Pathog 8:e1003081.

64. Varble A, Albrecht RA, Backes S, Crumiller M, Bouvier NM, Sachs D, Garcia-Sastre A, tenOever BR. 2014. Influenza A virus transmission bottlenecks are defined by infection route and recipient host. Cell Host Microbe 16:691-700.

65. Wasik BR, Voorhees IEH, Barnard KN, Alford-Lawrence BK, Weichert WS, Hood G, Nogales A, Martinez-Sobrido L, Holmes EC, Parrish CR. 2019. Influenza Viruses in Mice: Deep Sequencing Analysis of Serial Passage and Effects of Sialic Acid Structural Variation. J Virol 93.

66. Soh YS, Moncla LH, Eguia R, Bedford T, Bloom JD. 2019. Comprehensive mapping of adaptation of the avian influenza polymerase protein PB2 to humans. Elife 8.

67. Jones JC, Pascua PNQ, Fabrizio TP, Marathe BM, Seiler P, Barman S, Webby RJ, Webster RG, Govorkova EA. 2020. Influenza A and B viruses with reduced baloxavir susceptibility display attenuated in vitro fitness but retain ferret transmissibility. Proc Natl Acad Sci U S A 117:8593-8601.

68. Hu M, Yuan S, Ye ZW, Singh K, Li C, Shuai H, Fai N, Chow BK, Chu H, Zheng BJ. 2017. PAN substitutions A37S, A37S/I61T and A37S/V63I attenuate the replication of H7N7 influenza A virus by impairing the polymerase and endonuclease activities. J Gen Virol 98:364-373.

69. Lee LY, Zhou J, Koszalka P, Frise R, Farrukee R, Baba K, Miah S, Shishido T, Galiano M, Hashimoto T, Omoto S, Uehara T, Mifsud EJ, Collinson N, Kuhlbusch K, Clinch B, Wildum S, Barclay WS, Hurt AC. 2021. Evaluating the fitness of PA/I38T-substituted influenza A viruses with reduced baloxavir susceptibility in a competitive mixtures ferret model. PLoS Pathog 17:e1009527.

70. Goldhill DH, Yan A, Frise R, Zhou J, Shelley J, Gallego Cortes A, Miah S, Akinbami O, Galiano M, Zambon M, Lackenby A, Barclay WS. 2021. Favipiravir-resistant influenza A virus shows potential for transmission. PLoS Pathog 17:e1008937.

71. Cheung PP, Watson SJ, Choy KT, Fun Sia S, Wong DD, Poon LL, Kellam P, Guan Y, Malik Peiris JS, Yen HL. 2014. Generation and characterization of influenza A viruses with altered polymerase fidelity. Nat Commun 5:4794.

72. Imai M, Yamashita M, Sakai-Tagawa Y, Iwatsuki-Horimoto K, Kiso M, Murakami J, Yasuhara A, Takada K, Ito M, Nakajima N, Takahashi K, Lopes TJS, Dutta J, Khan Z, Kriti D, van Bakel H, Tokita A, Hagiwara H, Izumida N, Kuroki H, Nishino T, Wada N, Koga M, Adachi E, Jubishi D, Hasegawa H, Kawaoka Y. 2020. Influenza A variants with reduced susceptibility to baloxavir isolated from Japanese patients are fit and transmit through respiratory droplets. Nat Microbiol 5:27-33.

73. Lee JM, Huddleston J, Doud MB, Hooper KA, Wu NC, Bedford T, Bloom JD. 2018. Deep mutational scanning of hemagglutinin helps predict evolutionary fates of human H3N2 influenza variants. Proc Natl Acad Sci U S A 115:E8276-E8285.

74. Lakdawala SS, Jayaraman A, Halpin RA, Lamirande EW, Shih AR, Stockwell TB, Lin X, Simenauer A, Hanson CT, Vogel L, Paskel M, Minai M, Moore I, Orandle M, Das SR, Wentworth DE, Sasisekharan R, Subbarao K. 2015. The soft palate is an important site of adaptation for transmissible influenza viruses. Nature 526:122-5.

75. Murakami S, Horimoto T, Ito M, Takano R, Katsura H, Shimojima M, Kawaoka Y. 2012. Enhanced growth of influenza vaccine seed viruses in vero cells mediated by broadening the optimal pH range for virus membrane fusion. J Virol 86:1405-10.

76. DuBois RM, Zaraket H, Reddivari M, Heath RJ, White SW, Russell CJ. 2011. Acid stability of the hemagglutinin protein regulates H5N1 influenza virus pathogenicity. PLoS Pathog 7:e1002398.

77. Stevens J, Blixt O, Tumpey TM, Taubenberger JK, Paulson JC, Wilson IA. 2006. Structure and receptor specificity of the hemagglutinin from an H5N1 influenza virus. Science 312:404-10.

78. Byrd-Leotis L, Galloway SE, Agbogu E, Steinhauer DA. 2015. Influenza hemagglutinin (HA) stem region mutations that stabilize or destabilize the structure of multiple HA subtypes. J Virol 89:4504-16.

79. Zhong L, Wang X, Li Q, Liu D, Chen H, Zhao M, Gu X, He L, Liu X, Gu M, Peng D, Liu X. 2014. Molecular mechanism of the airborne transmissibility of H9N2 avian influenza A viruses in chickens. J Virol 88:9568-78.

80. Linster M, Schrauwen EJA, van der Vliet S, Burke DF, Lexmond P, Bestebroer TM, Smith DJ, Herfst S, Koel BF, Fouchier RAM. 2019. The Molecular Basis for Antigenic Drift of Human A/H2N2 Influenza Viruses. J Virol 93.

81. Reed ML, Yen HL, DuBois RM, Bridges OA, Salomon R, Webster RG, Russell CJ. 2009. Amino acid residues in the fusion peptide pocket regulate the pH of activation of the H5N1 influenza virus hemagglutinin protein. J Virol 83:3568-80.

82. Xiao C, Ma W, Sun N, Huang L, Li Y, Zeng Z, Wen Y, Zhang Z, Li H, Li Q, Yu Y, Zheng Y, Liu S, Hu P, Zhang X, Ning Z, Qi W, Liao M. 2016. PB2-588 V promotes the mammalian adaptation of H10N8, H7N9 and H9N2 avian influenza viruses. Sci Rep 6:19474.

83. Arai Y, Kawashita N, Elgendy EM, Ibrahim MS, Daidoji T, Ono T, Takagi T, Nakaya T, Matsumoto K, Watanabe Y. 2020. PA Mutations Inherited during Viral Evolution Act Cooperatively To Increase Replication of Contemporary H5N1 Influenza Virus with an Expanded Host Range. J Virol 95.

84. Diaz A, Marthaler D, Corzo C, Munoz-Zanzi C, Sreevatsan S, Culhane M, Torremorell M. 2017. Multiple Genome Constellations of Similar and Distinct Influenza A Viruses Co-Circulate in Pigs During Epidemic Events. Sci Rep 7:11886.

85. World Health Organization. 2018, posting date. Antigenic and genetic characteristics of zoonotic influenza viruses and candidate vaccine viruses developed for potential use in human vaccines, https://www.who.int/influenza/vaccines/virus/characteristics_virus_vaccines/en/.

86. Sun H, Xiao Y, Liu J, Wang D, Li F, Wang C, Li C, Zhu J, Song J, Sun H, Jiang Z, Liu L, Zhang X, Wei K, Hou D, Pu J, Sun Y, Tong Q, Bi Y, Chang KC, Liu S, Gao GF, Liu J. 2020. Prevalent Eurasian avian-like H1N1 swine influenza virus with 2009 pandemic viral genes facilitating human infection. Proc Natl Acad Sci U S A 117:17204-17210.

87. Zanin M, Duan S, Wong SS, Kumar G, Baviskar P, Collin E, Russell C, Barman S, Hause B, Webby R. 2017. An Amino Acid in the Stalk Domain of N1 Neuraminidase Is Critical for Enzymatic Activity. J Virol 91.

88. Zaraket H, Baranovich T, Kaplan BS, Carter R, Song MS, Paulson JC, Rehg JE, Bahl J, Crumpton JC, Seiler J, Edmonson M, Wu G, Karlsson E, Fabrizio T, Zhu HC, Guan Y, Husain M, Schultz-Cherry S, Krauss S, McBride R, Webster RG, Govorkova EA, Zhang JH, Russell CJ, Webby RJ. 2015. Mammalian adaptation of influenza A(H7N9) virus is limited by a narrow genetic bottleneck. Nature Communications 6.

89. Hu M, Yuan S, Ye ZW, Singh K, Li C, Shuai H, Fai N, Chow BKC, Chu H, Zheng BJ. 2017. PAN substitutions A37S, A37S/I61T and A37S/V63I attenuate the replication of H7N7 influenza A virus by impairing the polymerase and endonuclease activities. J Gen Virol 98:364-373.

90. Kawakami E, Watanabe T, Fujii K, Goto H, Watanabe S, Noda T, Kawaoka Y. 2011. Strand-specific real-time RT-PCR for distinguishing influenza vRNA, cRNA, and mRNA. J Virol Methods 173:1-6.

Figure Legends

Fig. 1. Virus characterization *in vitro*. (A) Sequence variations. Whole genomes of gamma viruses P4-PA-mixed, G15-HA1-mixed, G15-HA1-S210, and G15-HA1-N210 were obtained by next-generation sequencing. Amino-acid variations with frequencies ≥ 5% and reads ≥ 10 are shown in colored pie charts. H3 numbering was used for the HA protein. (B) HA activation pH values measured by syncytium assay. Viruses were inoculated into Vero cells at an MOI of 3 PFU/cell. Representative images are shown with the HA activation pH in bold. (C) Virus inactivation pH values. Viruses were treated with pH-adjusted PBS, re-neutralized, and subjected to measurement of residual virus infectivity by $TCID_{50}$. (D) Virus growth in MDCK cells. Viruses were inoculated into MDCK cells at an MOI of 2 PFU/cell. Cell-free culture supernatants were harvested at 6- and 8-hours post-infection (hpi) and titrated by $TCID_{50}$. All experiments were independently performed at least twice. *P* values were determined according to one-way ANOVA followed by a Tukey's multiple comparisons test. * and ** represent $P < 0.05$ and 0.01, respectively.

Fig. 2. *In vitro* transcription and replication of P4-PA-mixed and G15-HA1-S210. (A) Virus mRNA, cRNA, and vRNA accumulation after 4 hpi. (B) Virus mRNA, cRNA, and vRNA accumulation after 6 hpi. (C) Virus copies released into culture media. G15-HA1-S210 and P4-PA-mixed viruses were inoculated into MDCK cells at an MOI of 2 PFU/cell. At 4 and 6 hpi, the infected MDCK cells were lysed and harvested for total viral RNA. Virus specific mRNA, cRNA, and vRNA were quantified by two-step real-time reverse-transcription PCR using specific primers and normalized to GAPDH mRNA levels. Meanwhile, culture supernatants were harvested for quantification of virions released. Virions released from the cells were

quantified by real-time quantitative PCR using plasmid PHW2000-NP (G15-HA1-mixed) as a standard. Virus copies were quantified. *P* values were determined according to Welch's *t* test. *** represents $P < 0.001$.

Fig. 3. Infection of P4-PA-mixed, G15-HA1-mixed, and G15-HA1-S210 in inoculated donor ferrets. (A) Viral properties. Relative polymerase activity and HA stability for viruses are shown. (B) Ferret experimental caging. Viruses were intranasally inoculated into 3 donor ferrets per group on day 0. After one day, 3 naïve ferrets were introduced into the same cages and 3 into the adjacent cages. These ferrets were designated contact and airborne ferrets, respectively. Overall, there were 9 ferrets for each cubicle. (C) $TCID_{50}$ titers of virus in nasal washes from donor ferrets. Ferret nasal washes were collected every other day until day 14. Each symbol represents the virus titer of an individual sample. The bottom dashed lines represent the limit of detection. (D) Day of virus peak titer in donor ferrets. Each symbol represents the day that virus peak titer was observed in an individual donor ferret. (E) Virus peak titers in donor ferrets. Each symbol represents the virus peak titer in an individual donor ferret. (F) HAI titers of day-21 sera of donor ferrets. (G) Percent body weight of donor ferrets. Ferret body weight was monitored daily until day 14. *P* values were calculated using Mann-Whitney U test.

Fig. 4. P4-PA-mixed transmission, seroconversion, and frequency of single-nucleotide variants (SNVs) for nasal washes collected from transmitted ferrets. The ferret experiment was carried out as described in Fig. 3A. (A) Virus $TCID_{50}$ titers of nasal washes from contact and airborne ferrets. (B) HAI titers of day-21 sera of contact and airborne ferrets. (C) Frequencies of SNVs for nasal washes. The whole-genomes of nasal washes collected from contact and airborne ferrets infected or exposed with P4-PA-mixed were obtained by next-

generation sequencing. SNVs with frequencies ≥ 5% and reads ≥ 10 were read out. The listed SNVs met the following criteria: (1) resulted in protein sequence changes, and (2) appeared in nasal washes in each cubicle ≥ 2 times and/or frequencies greater than 30%. The frequencies of SNVs are represented by the colored boxes. Each column represents the SNVs for one ferret nasal wash. (D) The proportions of PA-S321 in P4-PA-mixed from the original inoculum and infected/exposed ferrets.

Fig. 5. Minor variant PA-S321 had enhanced polymerase activity. (A-C) Evaluation of polymerase activity of P4-PA-S321. The experiment was performed as described in Fig. 2. The transcription and replication of virus containing 100% variant PA-S321 were compared to those of G15-HA1-S210 and P4-PA-mixed. The experiments were independently performed twice. *P* values were determined according to one-way ANOVA followed by a Tukey's multiple comparisons test.

Fig. 6. G15-HA1-mixed transmission, seroconversion, and frequency of SNVs for nasal washes collected from transmitted ferrets. The ferret experiment was carried out as described in Fig. 3A, and frequency of SNVs were achieved and listed as described in Fig. 5C. (A) Virus $TCID_{50}$ titers of nasal washes from contact and airborne ferrets. (B) HAI titers of day-21 sera of contact and airborne ferrets. (C) Frequencies of SNVs for nasal washes. (D) The proportions of HA1- S210 in G15-HA1-mixed from the original inoculum and infected/exposed ferrets.

Fig. 7. Minor variant HA1-S210 had enhanced HA stability. (A-D) Virus HA activation pH values of isolates from G15-HA1-mixed, P4-PA-mixed, and G15-HA1-S210 infected/exposed

ferrets. Virus isolates from nasal washes were propagated in MDCK cells once. Syncytium assays were performed to measure the HA activation pH values of these isolates.

Fig. 8. G15-HA1-S210 transmission, seroconversion, and frequency of SNVs for nasal washes collected from transmitted ferrets. The ferret experiment was carried out as described in Fig. 3A, and frequency of SNVs were achieved and listed as described in Fig. 5C. (A) Virus $TCID_{50}$ titers of nasal washes from contact and airborne ferrets. (B) HAI titers of day-21 sera of contact and airborne ferrets. (C) Frequencies of SNVs for nasal washes. (D) The number of virus isolates from ferret nasal washes of donor, contact, and airborne ferrets.

Fig. 9. Relative polymerase activities and HA stabilities in ferrets. Relative polymerase activity and HA activation pH were compared for inoculated virus (left) and after airborne transmission in ferrets (right). Each symbol represents an individual ferret.

Table 1. Virus characteristics before and after infection and transmission in ferrets.

Virus characterization		P4-PA-mixed	G15-HA1-mixed	G15-HA1-S210	G15-HA1-N210
Genotype variations	HA1-210	S	85% N, 15% S	S	N
	PB2-648	M	L	L	L
	PA-271	T	P	P	P
	PA-321	92% N, 8%S	N	N	N
	PA-386	86% D, 14% N	D	D	D
Phenotype variations *in vitro*	HA activation pH [a]	5.5	5.8	5.6	5.8
	HA inactivation pH [b]	5.6	5.75	5.6	5.8
	Polymerase activity	lower	higher	higher	higher
	One-step growth	lower	higher	higher	highest
Donor ferrets	Virus growth ($\log_{10}$ $TCID_{50}$)	5.8 (± 1.2)	4.98 (± 0.25)	7.3 (± 0.67)	- [f]
	Number of isolates from ferrets [c]	9	9	9; 9 [d]	-
	Seroconversion	3/3	3/3	3/3; 3/3	-
	Day of peak titers	3 (± 2)	3	1	-
	Peak titers ($\log_{10}$ $TCID_{50}$)	6.7 (± 0.43)	6.2 (± 0.54)	7.3 (± 0.67)	-
	Major variants	PA-S321	HA1-S210	none	-
	HA activation pH range	5.5-5.6	5.5-5.9	5.5-5.6	-
Contact ferrets	Number of isolates from ferrets	9	9	9; 10	-
	Seroconversion	3/3	3/3	3/3; 3/3	-
	HA activation pH range	5.5-5.6	5.6-5.9	5.5-5.6	-
	Major variants	PA-S321	HA1-S210	none	-
Airborne ferrets	Number of isolates from ferrets	4	0	7; 3	-
	Days for virus shedding	8-14	-;	8-14; 2-6	-
	Seroconversion	3/3	2/3	3/3; 1/3	-
	Major variants	PA-S321	HA1-S210	sporadic	-
	Polymerase activity	higher & lower	higher	higher	-
	HA activation pH [e]	5.5-5.6	~5.6	5.5-5.6	-

[a] HA activation pH measured by syncytia assay.

[b] HA inactivation pH measured by treating viruses with indicated pH and titrating resulting virions by $TCID_{50}$.

[c] The Number of isolates is listed for those grown successfully in MDCK cells after recovery from ferrets in cubicle 1 and cubicle 2.

[d] Data for each virus is listed for each cubicle with the first X/Y number representing cubicle 1 and the second X/Y representing cubicle 2.

[e] HA activation pH of airborne-transmitted virus on first day of isolation.

[f] -, Not measured.

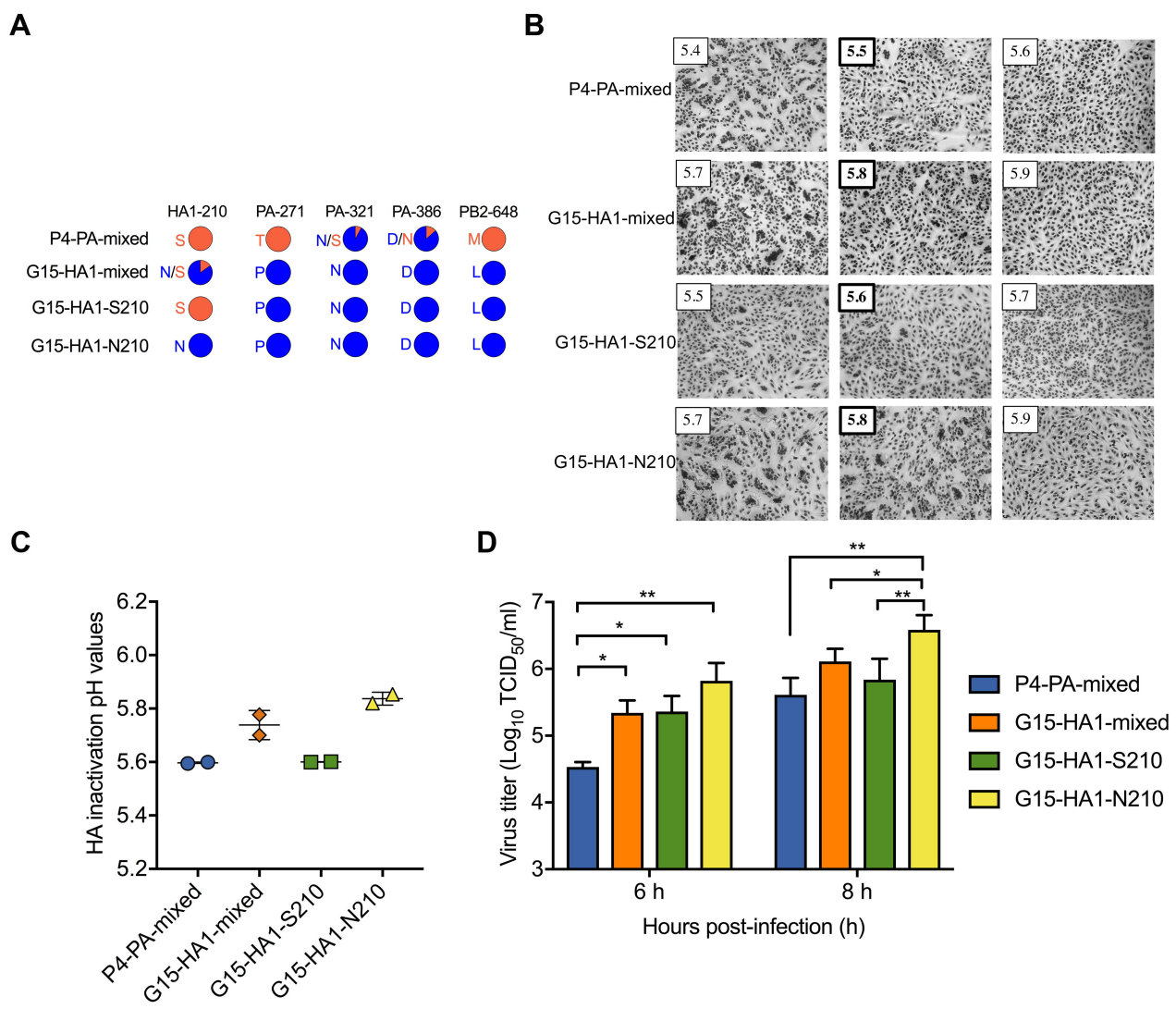
A
HA1-210
PA-271
PA-321
PA-386
PB2-648
P4-PA-mixed
S
T
N/S
D/N
M
G15-HA1-mixed
N/S
P
N
D
L
G15-HA1-S210
S
P
N
D
L
G15-HA1-N210
N
P
N
D
L
B
P4-PA-mixed
5.4
5.5
5.6
G15-HA1-mixed
5.7
5.8
5.9
G15-HA1-S210
5.5
5.6
5.7
G15-HA1-N210
5.7
5.8
5.9
C
HA inactivation pH values
6.2
6.0
5.8
5.6
5.4
5.2
P4-PA-mixed
G15-HA1-mixed
G15-HA1-S210
G15-HA1-N210
D
Virus titer (Log10 TCID50/ml)
7
6
5
4
3
*
*
**
*
**
**
6 h
8 h
Hours post-infection (h)
P4-PA-mixed
G15-HA1-mixed
G15-HA1-S210
G15-HA1-N210

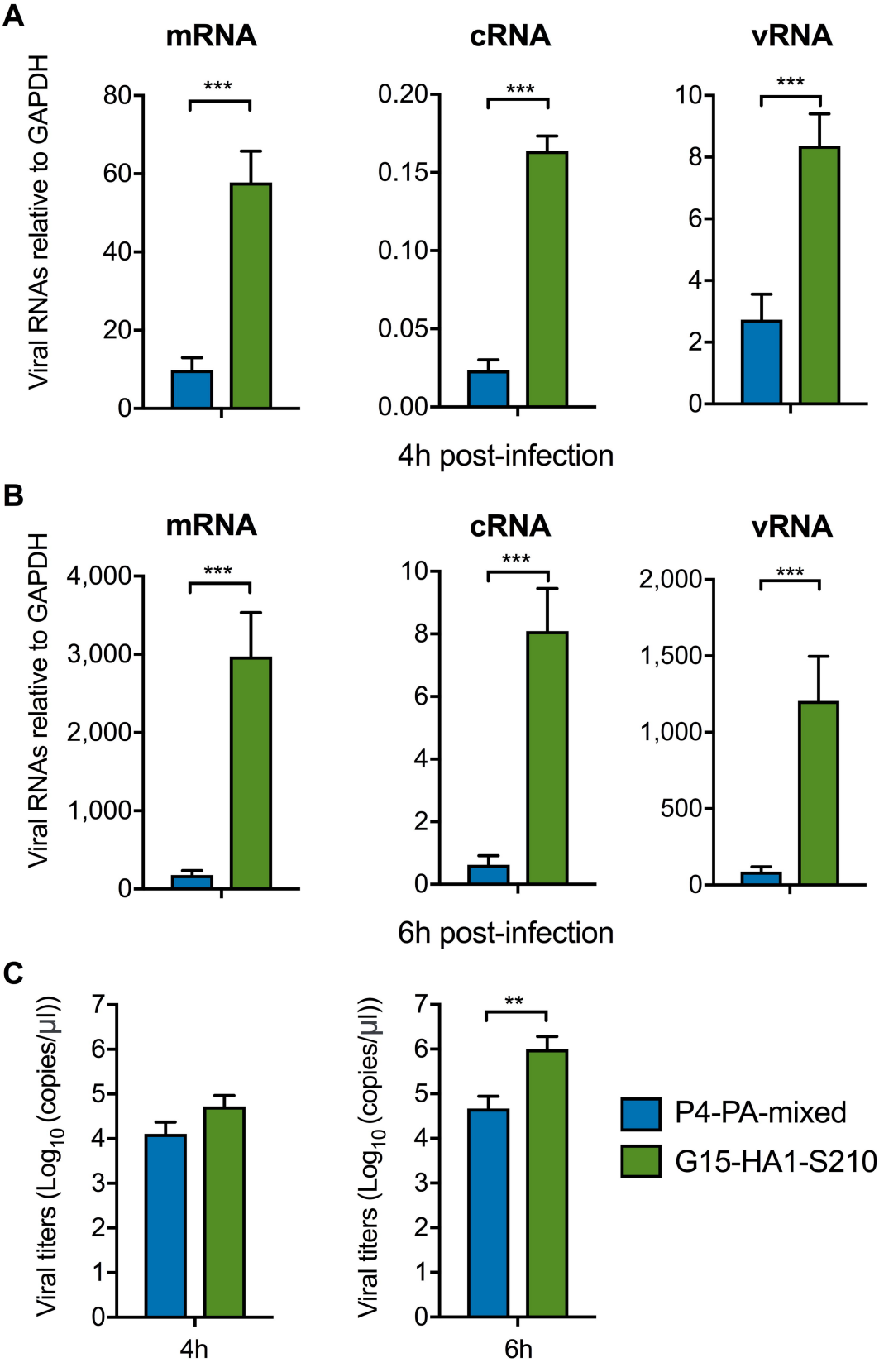
A
mRNA
cRNA
vRNA
Viral RNAs relative to GAPDH
***
80
60
40
20
0
0.20
0.15
0.10
0.05
0.00
10
8
6
4
2
4h post-infection
B
6h post-infection
4,000
3,000
2,000
1,000
500
1,500
C
Viral titers (Log10 (copies/µl))
**
7
1
4h
6h
P4-PA-mixed
G15-HA1-S210

A

	Relative polymerase activity	HA activation pH
P4-PA-mixed	Lower	5.5
G15-HA1-mixed	Higher	5.8
G15-HA1-S210	Higher	5.6

B

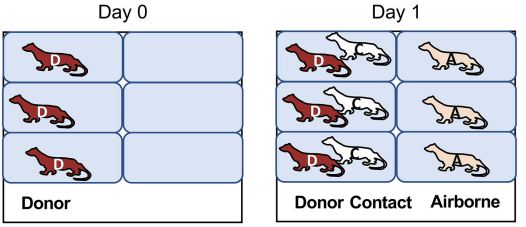

C

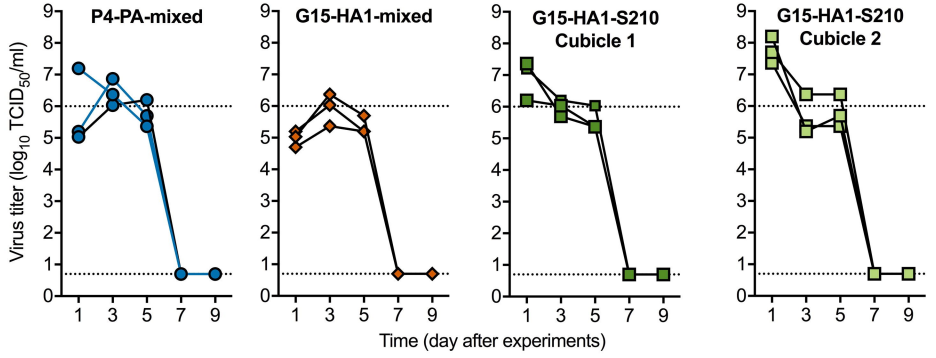

D

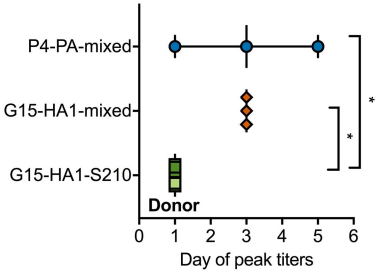

E

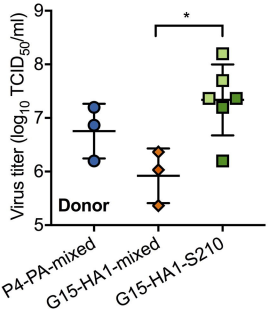

F

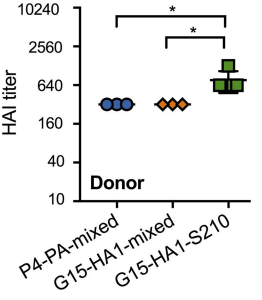

G

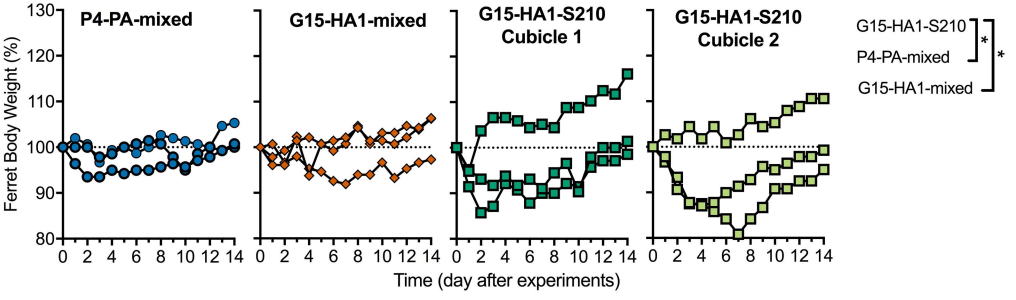

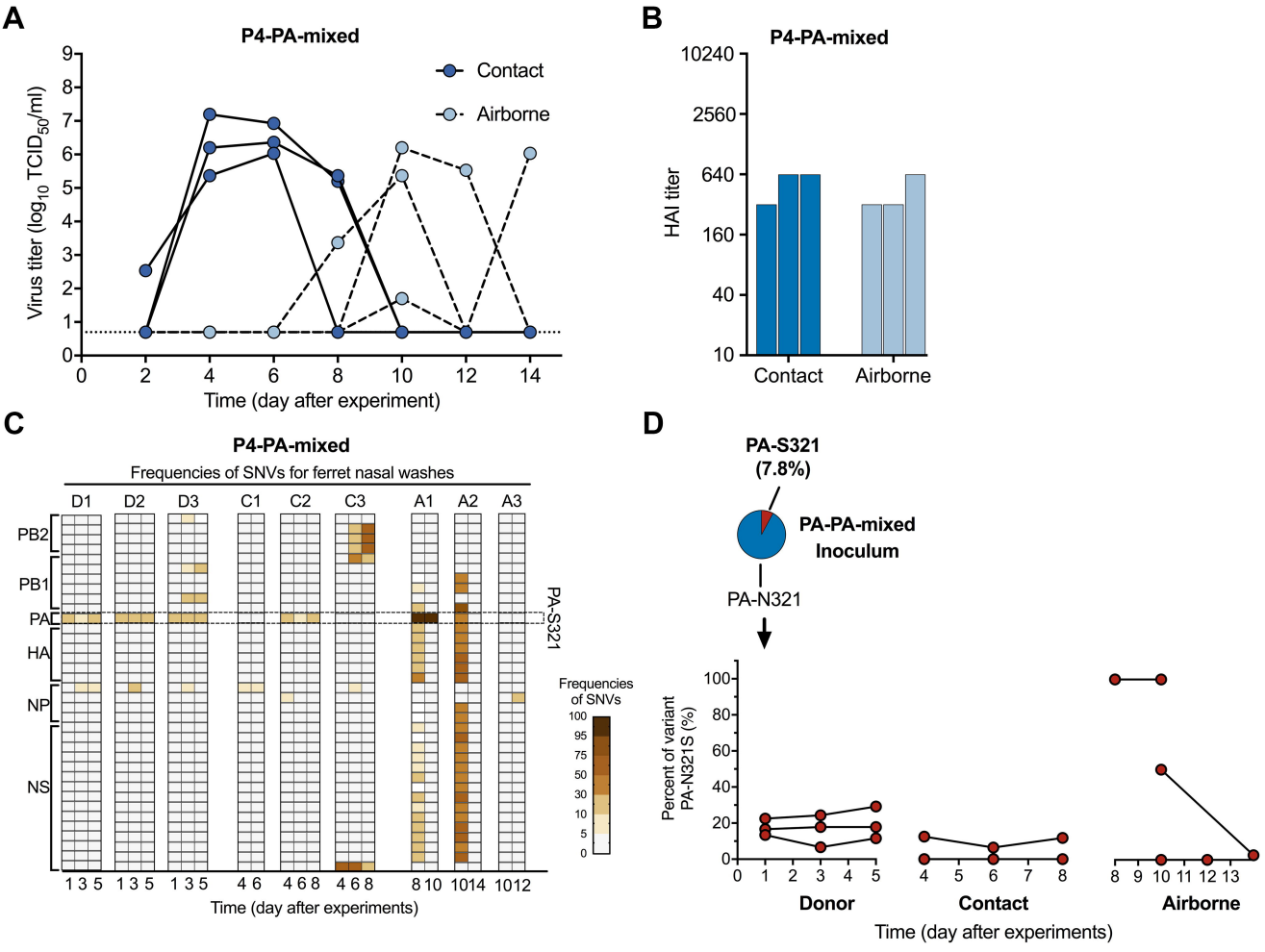
A
P4-PA-mixed
Contact
Airborne
Virus titer (log10 TCID50/ml)
Time (day after experiment)
B
P4-PA-mixed
HAI titer
10240
2560
640
160
40
10
Contact
Airborne
C
P4-PA-mixed
Frequencies of SNVs for ferret nasal washes
D1
D2
D3
C1
C2
C3
A1
A2
A3
PB2
PB1
PA
HA
NP
NS
PA-S321
Frequencies of SNVs
Time (day after experiments)
D
PA-S321
(7.8%)
PA-PA-mixed
Inoculum
PA-N321
Percent of variant PA-N321S (%)
Donor
Contact
Airborne
Time (day after experiments)

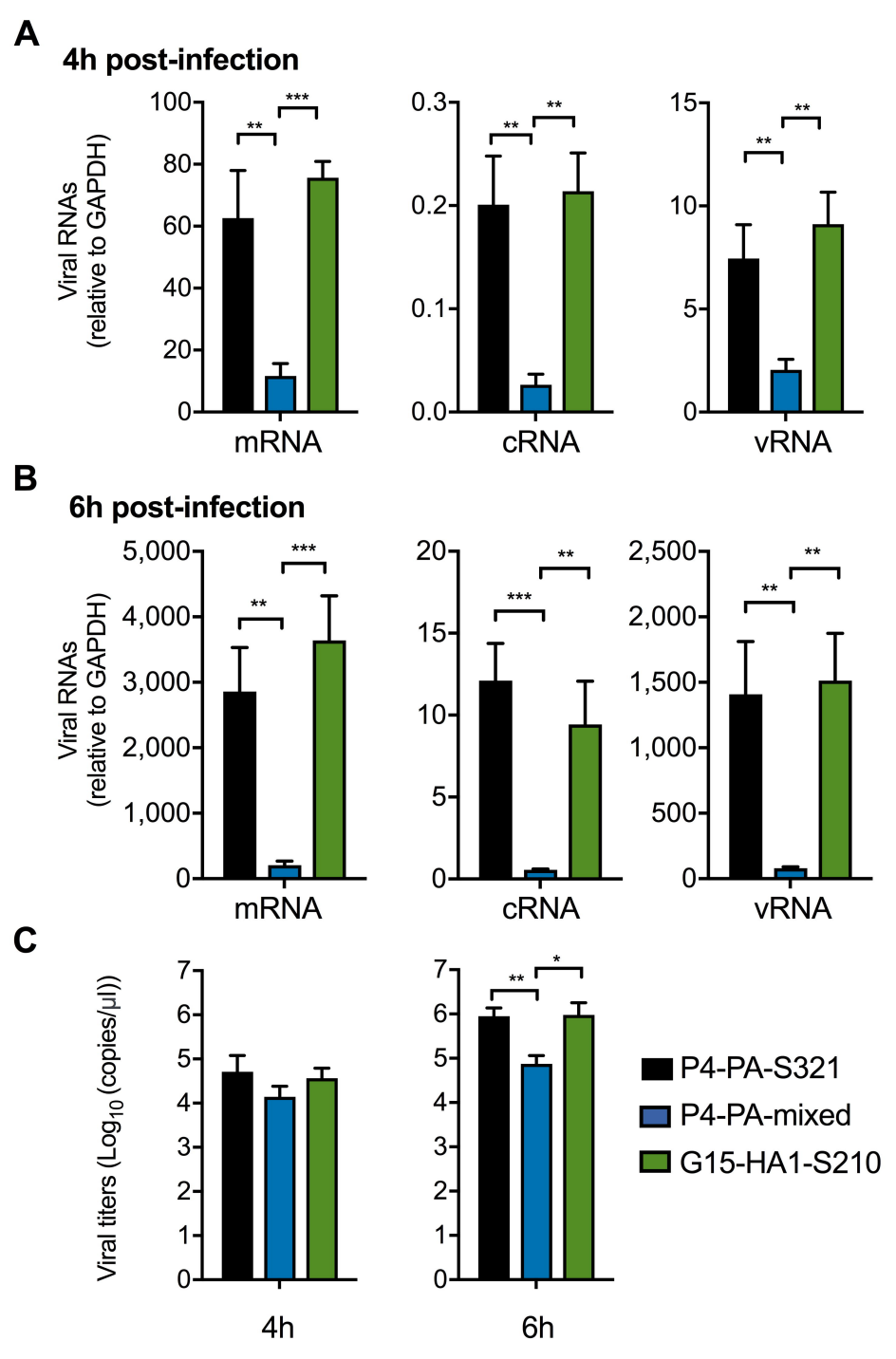
A
4h post-infection
Viral RNAs (relative to GAPDH)
100
80
60
40
20
0
**
***
mRNA
0.3
0.2
0.1
0.0
**
**
cRNA
15
10
5
0
**
**
vRNA
B
6h post-infection
Viral RNAs (relative to GAPDH)
5,000
4,000
3,000
2,000
1,000
0
**
***
mRNA
20
15
10
5
0
***
**
cRNA
2,500
2,000
1,500
1,000
500
0
**
**
vRNA
C
Viral titers (Log10 (copies/µl))
7
6
5
4
3
2
1
0
4h
**
*
6h
P4-PA-S321
P4-PA-mixed
G15-HA1-S210

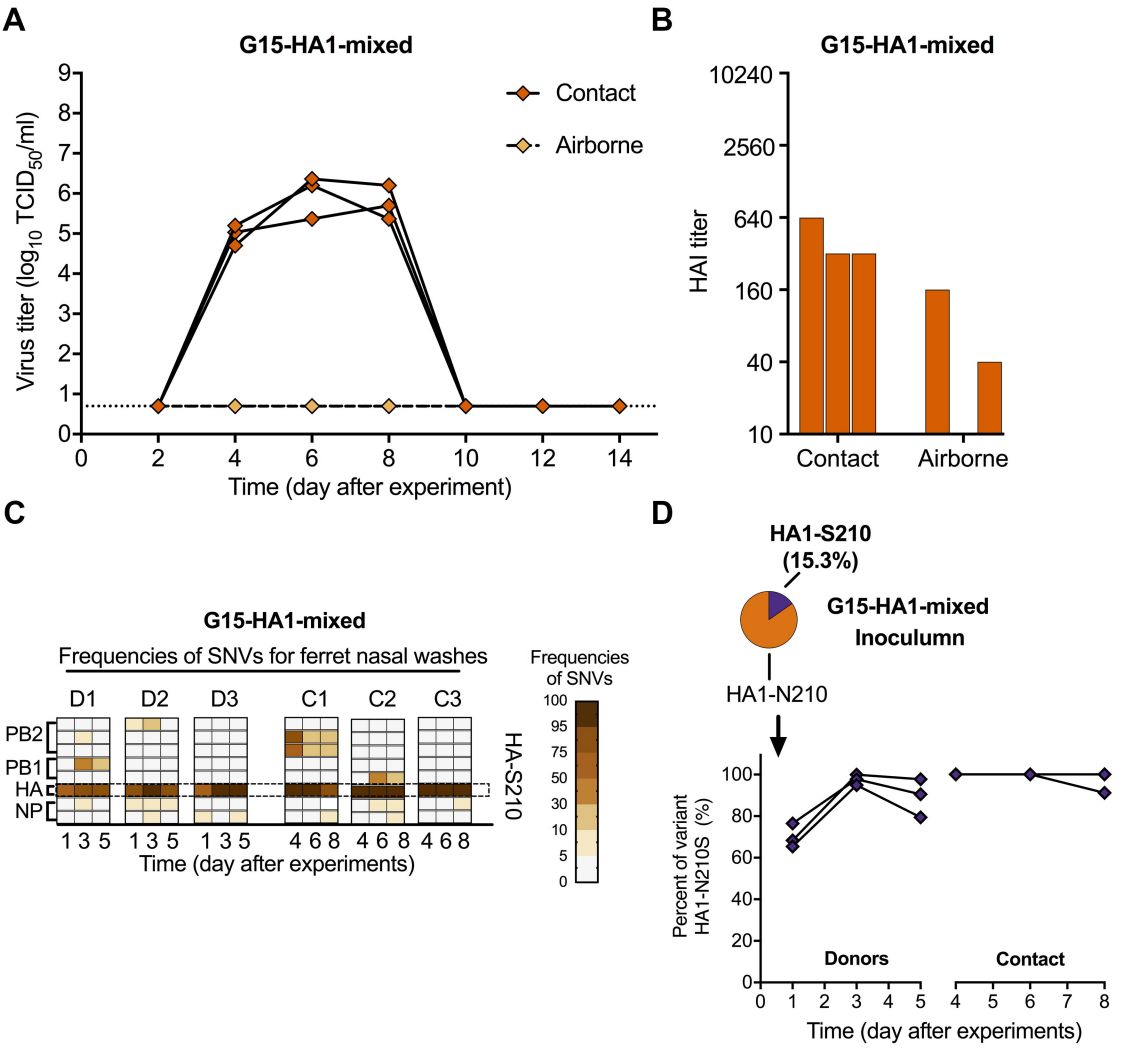
A
G15-HA1-mixed
Contact
Airborne
Virus titer (log10 TCID50/ml)
Time (day after experiment)
B
G15-HA1-mixed
HAI titer
10240
2560
640
160
40
10
Contact
Airborne
C
G15-HA1-mixed
Frequencies of SNVs for ferret nasal washes
D1
D2
D3
C1
C2
C3
PB2
PB1
HA
NP
HA-S210
Frequencies of SNVs
Time (day after experiments)
D
HA1-S210
(15.3%)
G15-HA1-mixed
Inoculumn
HA1-N210
Percent of variant HA1-N210S (%)
Donors
Contact
Time (day after experiments)

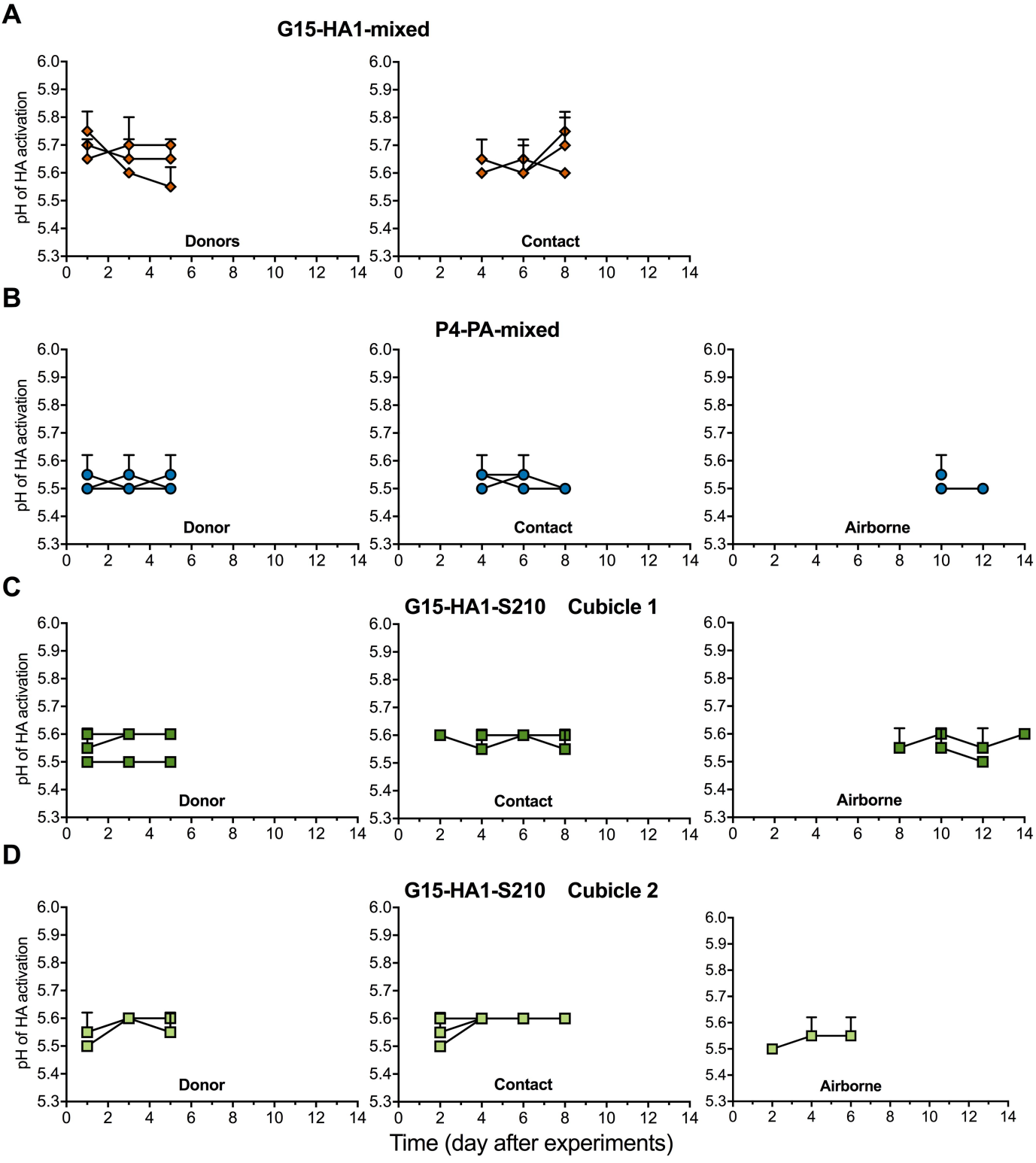
A
G15-HA1-mixed
pH of HA activation
Donors
Contact
B
P4-PA-mixed
Donor
Contact
Airborne
C
G15-HA1-S210 Cubicle 1
Donor
Contact
Airborne
D
G15-HA1-S210 Cubicle 2
Donor
Contact
Airborne
Time (day after experiments)

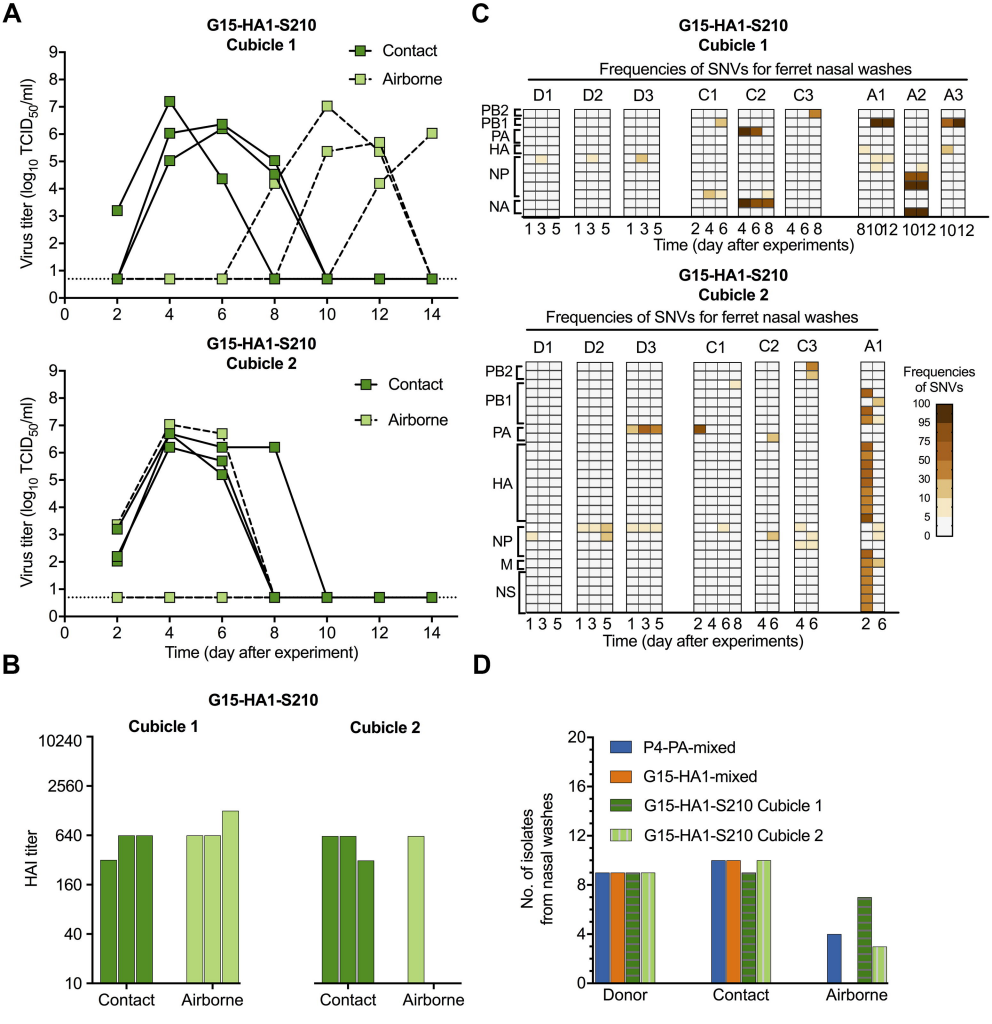
A
G15-HA1-S210
Cubicle 1
Contact
Airborne
Virus titer (log10 TCID50/ml)
G15-HA1-S210
Cubicle 2
Contact
Airborne
Virus titer (log10 TCID50/ml)
Time (day after experiment)
B
G15-HA1-S210
Cubicle 1
Cubicle 2
HAI titer
10240
2560
640
160
40
10
Contact
Airborne
Contact
Airborne
C
G15-HA1-S210
Cubicle 1
Frequencies of SNVs for ferret nasal washes
D1 D2 D3 C1 C2 C3 A1 A2 A3
PB2
PB1
PA
HA
NP
NA
Time (day after experiments)
G15-HA1-S210
Cubicle 2
Frequencies of SNVs for ferret nasal washes
D1 D2 D3 C1 C2 C3 A1
PB2
PB1
PA
HA
NP
M
NS
Frequencies of SNVs
100
95
75
50
30
10
5
0
Time (day after experiments)
D
P4-PA-mixed
G15-HA1-mixed
G15-HA1-S210 Cubicle 1
G15-HA1-S210 Cubicle 2
No. of isolates from nasal washes
Donor
Contact
Airborne

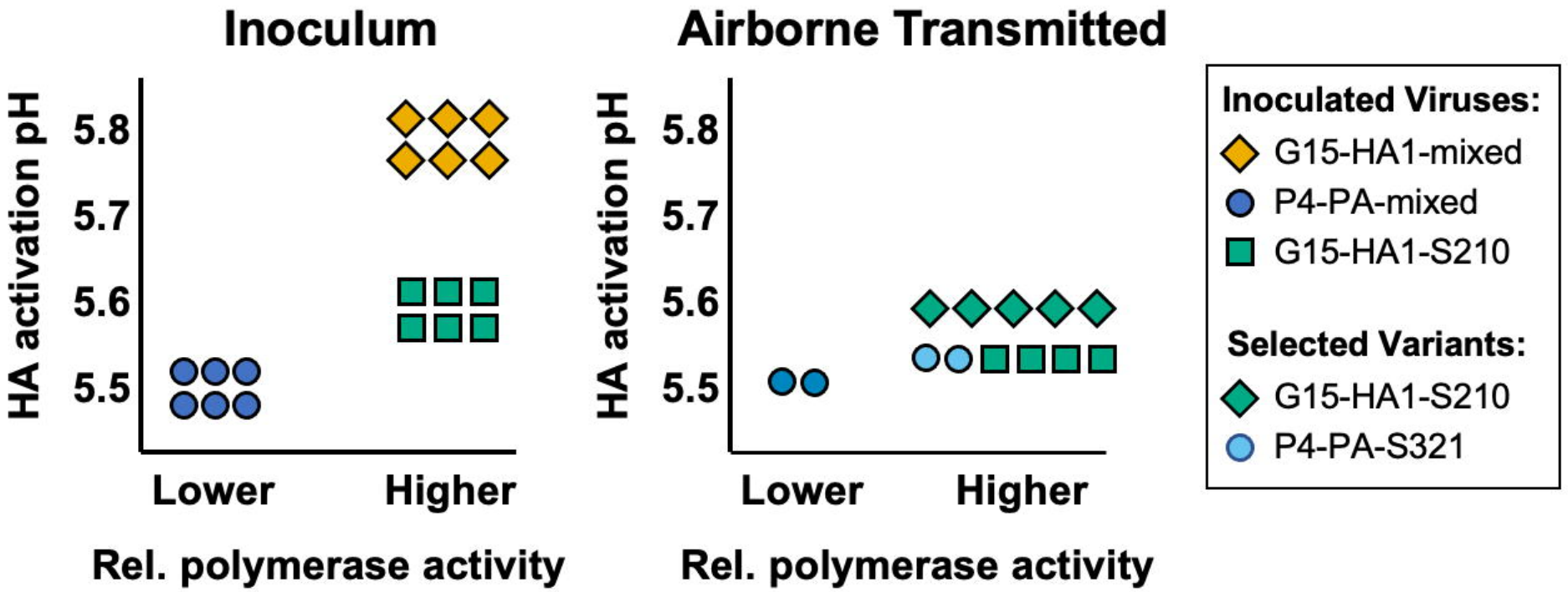
Inoculum
Airborne Transmitted
HA activation pH
5.8
5.7
5.6
5.5
Lower
Higher
Rel. polymerase activity
Inoculated Viruses:
G15-HA1-mixed
P4-PA-mixed
G15-HA1-S210
Selected Variants:
G15-HA1-S210
P4-PA-S321